AWARD NUMBER: W81XWH-14-2-0133

TITLE: Regulation of Heat Stress by HSF1 and GR

PRINCIPAL INVESTIGATOR: Yifan Chen

CONTRACTING ORGANIZATION:
Henry M. Jackson Foundation for the Advancement of Military Medicine
Bethesda, MD 20817

REPORT DATE: September 2016

TYPE OF REPORT: Annual

PREPARED FOR: U.S. Army Medical Research and Materiel Command
Fort Detrick, Maryland 21702-5012

REPORT DOCUMENTATION PAGE

Form Approved
OMB No. 0704-0188

1. REPORT DATE	**2. REPORT TYPE**	**3. DATES COVERED**
September 2016	Annual	15 Aug 2015 - 14 Aug 2016

4. TITLE AND SUBTITLE
Regulation of Heat Stress by HSF1 and GR

5a. CONTRACT NUMBER

5b. GRANT NUMBER
W81XWH-14-2-0133

5c. PROGRAM ELEMENT NUMBER

6. AUTHOR(S)
Yifan Chen

E-Mail: yifan.chen@usuhs.edu

5d. PROJECT NUMBER

5e. TASK NUMBER

5f. WORK UNIT NUMBER

7. PERFORMING ORGANIZATION NAME(S) AND ADDRESS(ES)
Uniformed Services University of the Health Sciences
4301 Jones Bridge Road
Bethesda, MD 20814

8. PERFORMING ORGANIZATION REPORT NUMBER

9. SPONSORING / MONITORING AGENCY NAME(S) AND ADDRESS(ES)

U.S. Army Medical Research and Materiel Command
Fort Detrick, Maryland 21702-5012

10. SPONSOR/MONITOR'S ACRONYM(S)

11. SPONSOR/MONITOR'S REPORT NUMBER(S)

12. DISTRIBUTION / AVAILABILITY STATEMENT

Approved for Public Release; Distribution Unlimited

13. SUPPLEMENTARY NOTES

14. ABSTRACT

The purpose of this project is to examine how activation of two cellular defense mechanisms involving heat shock transcription factor 1 (HSF1) and glucocorticoid receptor (GR) is associated with heat tolerance and heat acclimation. This relationship will be examined in cultured mouse skeletal muscle cells (task 1); in heat-tolerant versus -intolerant mice (task 2); and in heat-acclimated and unacclimatized mice (task 3). We have completed all the cell-based tests and performed molecular assays for task 1. This work has resulted in one manuscript (accepted). We have found that heat acclimation and moderate heat shock appear to have different effects on the mitochondrial morphology and fission protein in skeletal muscle cells. The signaling pathways involving HSF1 and GR are known to regulate mitochondrial function. Thus these findings suggest that mitochondrial dynamics may also serve as potential biomarkers indicating heat resistance and HA effect. In addition, in this second annual reporting period, we conducted animal experiments for tasks 2 and 3. The work of the project is progressing as projected.

15. SUBJECT TERMS
heat adaptation, heat intolerance, skeletal muscle, C2C12, myoblast, rodent

16. SECURITY CLASSIFICATION OF:			**17. LIMITATION OF ABSTRACT**	**18. NUMBER OF PAGES**	**19a. NAME OF RESPONSIBLE PERSON**
a. REPORT	**b. ABSTRACT**	**c. THIS PAGE**			USAMRMC
U	U	U	UU	50	**19b. TELEPHONE NUMBER** *(include area code)*

Table of Contents

1. Introduction

The cellular defense mechanisms mediated by heat shock factor 1 (HSF1) and glucocorticoid receptor (GR) are known to provide primary protection against immediate and prolonged stress. The purpose of this project is to examine the roles of the two systems involving HSF1 and GR in the regulation of heat tolerance and heat acclimation (HA), which remain poorly understood. We propose to assess effects of heat exposure and HA on activation of HSF1-GR systems in our cultured cell model of heat injury and mouse model of heat intolerance as well as in their normal counterparts. Findings from these studies should increase our understanding of potential mechanisms for heat intolerance and provide information useful for future research in heat injury prevention.

2. Keywords

hyperthermia, heat shock, heat injury, heat adaptation, rodent, skeletal muscle, C2C12, myotube, hsp, inflammation, cytokines, oxidative stress

3. Accomplishments

What were the major goals of the project?

The major goal of this project is to determine how heat tolerance and HA are associated with activation of two stress response systems (HSF1 and GR) under *in vitro* and *in vivo* conditions. As proposed, we will accomplish three tasks: 1) to examine the effects of HA on resistance to heat injury in C2C12 mouse skeletal muscle cells (August 15, 2014 – August 15, 2015); 2) to examine the relationship between activation of tissue HSF-GR and heat stress in heat-tolerant (TOL) versus -intolerant (INT) mice (August 15, 2014 – August 15, 2016); and 3) to examine the relationship between HSF-GR homeostasis and heat stress responses in TOL versus INT mice following HA (November 15, 2015 – August 15, 2017).

What opportunities for training and professional development did the project provide?

Nothing to Report

How were the results disseminated to communities of interest?

Nothing to Report

What was accomplished under these goals?

During this 2nd annual reporting period, we accomplished the following:
Task 1 - Completed all proposed experiments in C2C12 cells and, continued sample analysis/report preparation;
Task 2 - Conducted additional heat exposure experiments in TOL or INT mice and performed some tissue assays;
Task 3 - Conducted heat exposure experiments in HA mice

Our preliminary data continue to support the involvement of SHF1 and GR in heat stress and HA.

1) Expression of HSF1 and GR in skeletal muscles of TOL vs INT mice

We previously reported reduced expression of HSF1 and GR in the gastrocnemius muscles of INT mice compared to TOL mice one day after heat exposure. We recently repeated the measurements within one hour after heat exposure. We found that HSF1 and Hsp72 levels in the muscles of INT mice were higher compared to TOL mice (Figure 1). But the muscle GR and phosphorylated GR (p-GR) were lower in INT mice than in TOL mice. Furthermore, our preliminary results show that mitochondrial uncoupling proteins 2 and 3 (UCP2, UCP3) were down-regulated in in the gastrocnemius muscles of INT mice compared to TOL mice. UCPs separate oxidative phosphorylation from ATP synthesis with energy dissipated as heat, and regulate mitochondrial thermogenesis and mitochondria-derived reactive oxygen species, which likely play a role in heat stress response. Both HSF1 and GR may directly or indirectly affect UCPs. For example, glucocorticoid can activate the transcription of UCP3 gene.

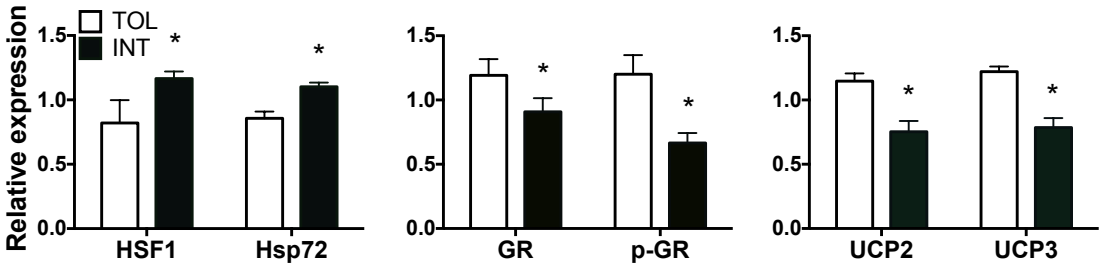

Figure 1. Comparison of HSF1, Hsp72, GR, p-GR, UCP3 and UCP2 expression relative to actin in the gastrocnemius muscles of TOL and INT mice. Muscle samples were obtained 30-60 minutes after heat exposure. Data are expressed as mean ± SD. * $p < 0.01$ versus TOL.

2) Effects of HA on expression of HSF1 and GR

We examined the in vitro effects of HA on HSF1 and GR, as proposed for Task 1. Our results show that HA caused rapid expression of HSF1 (Figure 2 left) but gradual up-regulation of GR (Figure 2 right) in C2C12 mouse skeletal muscle cells.

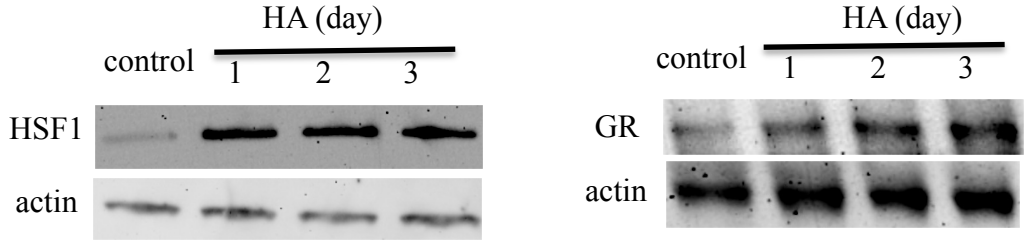

Figure 2. Western blot analysis of the HSF1 (left) and GR (right) in C2C12 cells (mouse skeletal muscle cell line). HA cells were exposed to 39.5 °C for 3 hours each day for 3 days. Control cells and HA cells (when not being incubated at 39.5 °C) were maintained at 37 °C for 3 days.

We also assessed the *in vivo* effects of HA. HA significantly reduced hyperthermic response in mice during heat exposure. Specifically, mice underwent two heat exposure tests, one before and one after HA or control protocol. HA mice had significantly lower peak core body temperature (Tc) during the second heat test, when compared to that during the first heat test (Figure 3). No differences in peak Tc were found between two heat tests in control mice.

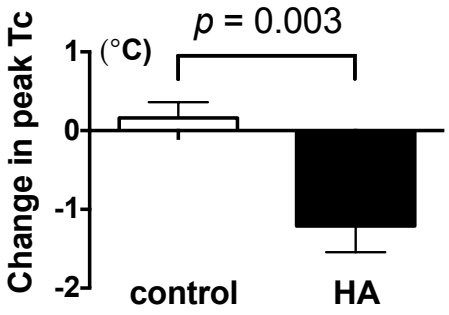

Figure 3. Changes in peak Tc between two heat tests in control and HA mice (n = 9 per group). After the first heat exposure test, HA mice were exposed to 33 °C in an environmental chamber for 3 hours daily for consecutive 10 days, while control mice were maintained at 21 °C. Subsequently the second heat exposure test was conducted in control and HA mice. Changes in peak Tc were obtained by subtracting peak Tc values during heat test 1 from that during heat test 2 of each animal.

We found that HA mice had increased expression of phosphorylated GR and HSF1 in their gastrocnemius muscles compared to control mice (Figure 4). But no significant changes in GR were detected between control and HA mice.

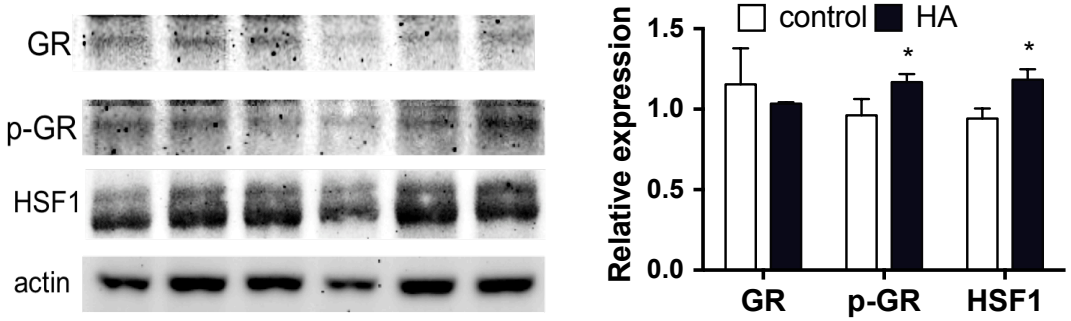

Figure 4. Representative western blot (left) and quantitative analysis (right) of GR, phosphorylated GR (p-GR) and HSF1 expression relative to actin in the gastrocnemius muscles of control and HA mice. Actin was used as loading control. * $p < 0.05$ versus control, n = 3 per group.

Furthermore, we examined GR and HSF1 contents in the cytosol, mitochondria, and nucleus of the skeletal muscles. We found that HA mice had increased expression of GR and HSF1 in the cytosol and nuclear fractions, and increased expression of GR (not HSF1) in the mitochondrial fraction from the gastrocnemius muscle tissues (Figure 5).

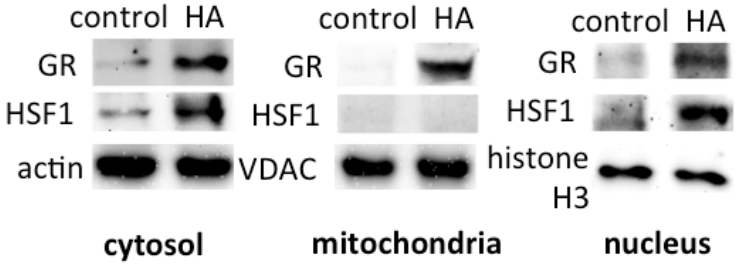

Figure 5. Representative western blot of GR and HSF1 in the cytosol, mitochondrial and nuclear fractions from the gastrocnemius muscles of control and HA mice.

Together, these results suggest that HSF1 and GR are indeed sensitive to heat stress as well as HA. Mitochondria in skeletal muscles are likely the target organelle of acute severe and repeated mild thermal stressors. We recently found that resistance of muscle cells against heat injury is associated mitochondrial integrity (see Appendix). Several key mitochondrial mediators, including UCPs and fission mediator Drp1, affected by heat stress and HA affect are subject to regulations by HSF1 and GR-dependent signaling pathways. The study of this complex system presents a new approach to identification of biomarkers for detection of susceptibility to heat injury.

What do you plan to do during the next reporting period to accomplish the goals and objectives?

We plan to finish the experiments of INT vs TOL mice (Task 2) before the end of February 2017 and HA vs control mice (Task 3) before the end of May 2017. Subsequent 8-9 weeks will be needed to complete sample processing, data analysis and report preparation for each Task. These studies of Tasks 2 and 3 are expected to verify association between activation of HSF-GR signaling and heat tolerance in vivo. The information will help to achieve the ultimate goal of this study - to identify novel key mediators of heat stress responses as biomarkers that can be used to assess heat tolerance in humans.

4. Impact

What was the impact on the development of the principal discipline(s) of the project?
Nothing to Report
What was the impact on other disciplines?
Nothing to Report
What was the impact on technology transfer?
Nothing to Report
What was the impact on society beyond science and technology?
Nothing to Report

5. Changes/Problems

In an effort to make potential findings of this project more widely applicable, we conducted a pilot study to examine the thermal response of female mice to heat exposure. Female mice showed a different thermal response profile when compared to males. Heat exposure induced a triphasic (physiological zone, thermo-neutral zone and reactive hyperthermia) response of Tc in male, but a biphasic (physiological and thermo-neutral) response of Tc in female mice (Figure 6). That is, unlike male mice, female mice were able to maintain their peak Tc around the ambient temperature (thermo-neutral) inside a heat chamber throughout heat exposure without reactive hyperthermia (Tc: 0.5 °C or higher above Ta). We also compared the changes in Tc in response to heat exposure in female mice during three different phases in an estrous cycle (diestrous: n = 5, proestrous: n = 6, extrous: n = 5) and found no significant differences in their baseline Tc (36.3 ± 1.1, 37.1 ± 0.7 and 37.3 ± 0.7 °C) or peak Tc (40.2 ± 0.3, 40.1 ± 0.2 and 40.1 ± 0.1 °C) during heat exposure across the three phases. Furthermore, like female mice, castrated male mice kept their Tc within the thermo-neutral range and did not experience reactive hyperthermia during heat exposure. These results suggest that heat-induced reactive hyperthermia, which ultimately leads to heat intolerance and heat injury, is at least in part mediated by male sex hormone.

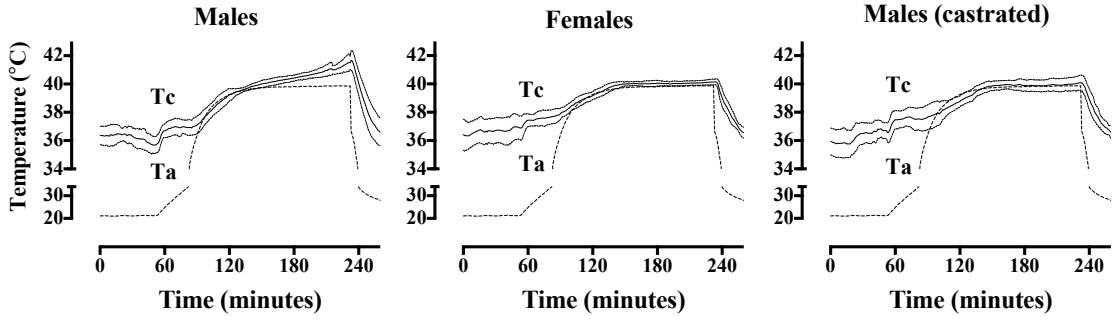

Figure 6. Body core temperature (Tc) of C57BL/6J mice and corresponding ambient temperature (Ta, dashed line) during heat exposure. Tc values are presented as mean (solid line) ± SD (dot line). Male: n = 12; female: n =16; castrated male: n = 8.

These novel findings raise at least two key questions that may complicate our effort to understand the involvement of HSF1 and/or GR in the regulation of response to heat stress in the current project: 1) whether sex hormones (e.g. testosterone) affect HSF1 (PMID: 24599545) and/or GR (PMID: 173192) signaling pathways; and 2) whether there is relationship between heat-induced hyperthermic response and testosterone level (testosterone itself is a biomarker for predicting susceptibility to heat injury). These challenging questions should also be potentially rewarding. A study of effects of low- and high-dose testosterone replacement therapy on thermoregulatory response to heat shock in castrated male mice (n = 8 each dose group) would provide valuable information. The study is expected to cause ~ 8 weeks of delays to this project if approved.

6. Products

One manuscript: "Tianzheng Yu, Patricia Deuster, Yifan Chen. Role of dynamin-related protein 1-mediated mitochondrial fission in resistance of mouse C2C12 myoblasts to heat injury. *The Journal of Physiology* (1st revision under review)". The manuscript describes several discoveries in the studies for Task 1. We found that HA and moderate heat shock appear to have different effects on the mitochondrial morphology and fission protein Drp1 in skeletal muscle cells. Specifically, HA causes mitochondrial elongation in C2C12 cells and mouse gastrocnemius muscles and reduces Drp1 in mitochondrial fractions from the cells and muscle tissue. In contrast, exposure to heat shock leads to apoptotic response along with mitochondrial fragmentation and Drp1 activation in C2C12 cells (see Appendix). Both the heat shock and glucocorticoid pathways are known to regulate mitochondrial function. Our assessment of HSF1-GR activation in heat-exposed and HA-treated C2C12 cells is still ongoing.

7. Participants & Other Collaborating Organizations

What individuals have worked on the project?

Name: Yifan Chen
Project Role: PI
Researcher Identifier (ORCID ID): 0000-0003-1388-9200
Nearest person month worked:
Contribution to Project: performed work in project management, provided assistance in experiments and prepared/revised the above manuscript.

Name: Tianzheng Yu
Project Role: Senior Scientist
Researcher Identifier (e.g. ORCID ID): N/A
Nearest person month worked: 21
Contribution to Project: conduced animal experiments, processed tissue samples, performed assays and helped preparing/revising the above manuscript.

Has there been a change in the active other support of the PD/PI(s) or senior/key personnel since the last reporting period?

Nothing to Report

What other organizations were involved as partners?

Nothing to Report

8. Special Reporting Requirements

None

9. Appendix

Role of dynamin-related protein 1-mediated mitochondrial fission in resistance of mouse C2C12 myoblasts to heat injury

Tianzheng Yu, Patricia Deuster, Yifan Chen

Department of Military and Emergency Medicine, Uniformed Services University of the Health Sciences, Bethesda, MD 20814, USA

Running title: Mitochondria and heat stress

Correspondence:
Yifan Chen, Ph.D.
Department of Military and Emergency Medicine
Uniformed Services University of the Health Sciences
4301 Jones Bridge Road
Bethesda, MD 20814
USA
Tel: 301-295-4526
Fax: 301-295-6773
Email: yifan.chen@usuhs.edu

KEY WORDS: apoptosis, heat acclimation, heat stress, mitochondrial dynamics, mitochondrial division inhibitor-1, reactive oxygen species, skeletal muscle

Key points

- Understanding how skeletal muscles respond to high temperatures may help develop strategies for improving exercise tolerance and preventing heat injury.
- Mitochondria regulate cell survival by constantly changing their morphology through fusion and fission in response to environmental stimuli. Little is known about the involvement of mitochondrial dynamics in tolerance of skeletal muscle against heat stress.
- Mild heat acclimation and moderate heat shock appear to have different effects on the mitochondrial morphology and fission protein Drp1 in skeletal muscle cells. Mitochondrial integrity plays a key role in cell survival under heat stress.

Abstract

The regulation of mitochondrial morphology is closely coupled to cell survival during stress. We examined changes in the mitochondrial morphology of mouse C2C12 skeletal muscle cells in response to heat acclimation and heat shock exposure. Acclimated cells showed a greater survival rate during heat shock exposure than non-acclimated cells, and were characterized by long interconnected mitochondria and reduced expression of dynamin-related protein 1 (Drp1) for their mitochondrial fractions. Exposure of C2C12 muscle cells to heat shock led to apoptotic death featuring activation of caspase 3/7, release of cytochrome c and loss of cell membrane integrity. Heat shock also caused excessive mitochondrial fragmentation, loss of mitochondrial membrane potential, and production of reactive oxygen species in C2C12 cells. Western blot and immunofluorescence image analysis revealed translocation of Drp1 to mitochondria from the cytosol in C2C12 cells exposed to heat shock. Mitochondrial division inhibitor 1 or Drp1 gene silencer reduced mitochondrial fragmentation and increased cell viability during exposure to heat shock. These results suggest that Drp1-dependent mitochondrial fission may regulate susceptibility to heat-induced apoptosis in muscle cells and that Drp1 may serve as a target for the prevention of heat-related injury.

Abbreviations. AR, aspect ratio; Drp1, dynamin-related protein 1; DHE, dihydroethidium; FF, Form factor; GFP, green fluorescence protein; HA, heat acclimation; HSF1, heat shock transcription factor 1; HSPs, heat shock proteins; IMF, intermyofibrillar; Mfn1, mitofusin 1; Mfn2, mitofusin 2; Mdivi-1, mitochondrial division inhibitor 1; OPA1, optic atrophy 1; ROS, reactive oxygen species; SS, subsarcolemmal; TEM, transmission electron microscope; TMRE, tetramethylrhodamine ethyl ester;

Introduction

Skeletal muscle, which makes up ~40-50% of the body mass in mammals, generates significant amounts of heat during contraction (Block, 1994). Muscle temperature can exceed 40 °C during exercise (Taylor *et al.*, 1998; Drust *et al.*, 2005). Understanding the regulation of muscle function under high temperatures may help develop strategies for improving performance and preventing injury. Exposure to a temperature above the physiological range can produce both detrimental and beneficial effects on muscle health. In general, acute exposure to very high temperatures can cause apoptotic damage in muscle cells (Islam *et al.,* 2013) and muscle injury in animals (Abdelnasir *et al.*, 2014), whereas frequent exposures to moderately high temperatures or heat acclimation (HA) may protect muscle cells against a subsequent severe heat insult (Monastyrskaya *et al.*, 2003; Liu & Brooks, 2012). In fact, HA has also been tested for cross-tolerance or protection against other pathological conditions (Horowitz *et al.*, 2015). Interestingly, HA has been shown to protect against obesity-induced insulin resistance by increasing heat shock protein 72 in skeletal muscles of mice (Chung *et al.*, 2008; Gupte *et al.*, 2009). How muscle cells paradoxically respond to mild versus severe heat stress remains poorly understood. The majority of studies of the adaptation and resistance of muscle cells to heat have focused on mechanisms involving heat shock transcription factor 1 (HSF1) and heat shock proteins (HSPs) (Tetievsky *et al.*, 2008; Abdelnasir *et al.*, 2014). Emerging evidence suggests that cellular organelles, including mitochondria, endoplasmic reticulum, lysosomes and the Golgi apparatus, serve key roles in stress/damage-sensing and apoptosis signaling. How they respond to the disruption of cellular homeostasis by high temperatures may ultimately determine the fate of stressed cells (Ferri & Kroemer, 2001).

Mitochondria regulate cell survival and coordinate cell-wide stress responses by constantly changing their morphology through fusion and fission in response to energy demands and environmental stimuli (Hoppins & Nunnari, 2012; Youle & van der Bliek, 2012). Disruption in these processes causes mitochondrial dysfunction, and leads to the pathogenesis of various acute and chronic diseases (Archer, 2013). High temperatures indeed affect mitochondrial function, and impair mitochondrial electron transport; this condition also induces the production of reactive oxygen species (ROS) under *in vitro* (Wang *et al.*, 2013) and *in vivo*

(Qian *et al.*, 2004) conditions. Altered mitochondrial morphology has also been observed in heat shock-exposed cultured mouse embryonic fibroblasts (Sanjuan Szklarz & Scorrano, 2012). How changes in mitochondrial morphology might affect resistance of cultured muscle cells, in particular C2C12 myoblasts, to heat is largely unexplored.

In mammals, mitochondrial morphology is coordinately regulated by several GTPases, dynamin-related protein 1 (Drp1) for fission and mitofusin isoforms (Mfn1 and 2), and optic atrophy1 (OPA1) for fusion, respectively (Ishihara *et al.*, 2006). The overall morphology and shape of mitochondria are determined by the balance between mitochondrial fission and fusion activities (Hoppins & Nunnari, 2012; Youle & van der Bliek, 2012; Archer, 2013). The role of mitochondrial dynamics proteins in responses to HA and heat stress has yet to be determined.

In this study, we investigated changes in mitochondrial morphology and dynamics of C2C12 mouse skeletal muscle cells exposed to HA or lethal heat shock. We discovered that HA-induced resistance of these cells against heat injury is associated with mitochondrial elongation mediated by down-regulation of the fission protein, Drp1. We demonstrate that exposing C2C12 cells to heat shock causes cell damage characterized by excessive mitochondrial fragmentation with increased recruitment of Drp1 to mitochondria. We further show that inhibition of mitochondrial fission by mitochondrial division inhibitor (Drp1 translocation blocker) Mdivi-1 or by Drp1 gene silencer protects mitochondrial morphology and prevents cell injury during exposure to heat shock. Together our work reveals a novel mechanism regulating resistance of C2C12 cells to heat stress, which may have relevance to heat injury prevention.

Methods

Cell culture, myogenic differentiation, heat acclimation and heat shock

The mouse skeletal myoblast cell line C2C12 was recently purchased from ATCC (ATCC® CRL-1772™) and was maintained at 37 °C in DMEM containing 10% fetal bovine serum, 100-units/ml penicillin and 100-µg/ml streptomycin. Myogenic differentiation was initiated

upon reaching ~80% confluence by switching the cells to DMEM containing 2% horse serum supplemented with 1μM insulin. For heat acclimation, cells were placed in an incubator preset at 39.5 °C for 3 hours per day for 3 days. Control cells and HA cells (when not being incubated at 39.5 °C) were maintained at 37 °C for 3 days. After the 3-day incubation, cells were tested for cell viability during exposure to heat shock. For heat shock, cells were maintained in an incubator preset at 43 °C for indicated times. Immediately after heat shock, cells were harvested for subsequent assays.

Mouse heat acclimation protocol

Mice (6-8 weeks old male C57BL/6J) were purchased from Jackson Laboratories (Bar Harbor, ME) and maintained in a temperature-controlled (21 °C) animal facilities at the Uniformed Services University (USU), with 12-hour light/dark cycle and free access to food & water. After arrival, all the mice were given one week to recover. Heat acclimation was initiated by exposing the mice to 33 °C in an environmental chamber from 8-11 AM (3 hours/day) for consecutive 10 days. Control mice were maintained at room temperature (21 °C) all the time. All procedures were approved by the USU Institutional Animal Care and Use Committee.

Transmission electron microscope (TEM) analysis of mitochondria in mouse skeletal muscle

Immediately after heat or sham exposure, mice were perfusion fixed under isoflurane anesthesia. The gastrocnemius muscle was removed and incubated in fixative (5% formaldehyde, 2% glutaraldehyde in 0.1M PBS, pH7.4) overnight. The samples were then sent to the Biomedical Instrument Center at USU for a standard TEM preparation procedure. The gastrocnemius muscle comprises a mixture of type I (mitochondria-rich) and type II (mitochondria-poor) muscle fibers (Mishra *et al.*, 2015). For comparison, only mitochondria enriched fibers were selected and areas presenting all the classical structures of sarcomere were imaged. For each animal, six to eight muscle fibers were analyzed, a total of 200 subsarcolemmal (SS) and 200 intermyofibrillar (IMF) mitochondria were individually traced by using NIH developed ImageJ software quantify the following morphological and shape

descriptors (Picard *et al.*, 2013): surface area, perimeter, circularity (4π·(surface area/perimeter2)) and Feret's diameter (longest distance between any two points within a given mitochondrion). Form factor (FF), a measure sensitive to the complexity and branching aspect of mitochondria, was calculated as perimeter/(4π·surface area) and aspect ratio (AR), a measure of the “length to width ratio”, was calculated as major axis/minor axis.

Cell viability and cell death assays

Cell viability was determined by trypan blue exclusion test with Bio-Rad TC20 automated cell counter per manufacturer's instruction. Caspase activity was measured by CellEvent™ Caspase-3/7 Green detection reagent (Molecular Probes), and dead cells were detected by using an Annexin V Alexa Fluor® 488 apoptosis kit (Molecular Probes).

Mitochondrial morphology analysis and membrane potential and ROS measurement

Mitochondria were labeled with CellLight Mitochondria-GFP (Molecular Probes) or visualized bysCMXRos (Invitrogen) staining. Quantitative analyses of mitochondrial morphology and Drp1 subcellular distribution were performed using ImageJ software (NIH Image) (Yu *et al.*, 2014). Mitochondrial membrane potential was evaluated with Tetramethylrhodamine ethyl ester (TMRE, Molecular Probes) and ROS levels were detected by using dihydroethidium, a fluorescent probe (DHE; Invitrogen), as described previously (Yu *et al.*, 2014).

Fluorescence microscopy

Fluorescence images were viewed and acquired with a Leica AF6000 epifluorescence microscope, which was equipped with a digital microscope camera. Excitation/emission wavelengths were 358/461 nm for blue fluorescence (4',6-diamidino-2-phenylindole, DAPI), 480/535 nm for green fluorescence (GFP, annexin V, Alexa 488, MitoTracker Green FM and

caspase-3/7 Green), and 555/613 nm for red fluorescence (MitoTracker Red, TMRE, ethidium, and Alexa 594).

Mitochondria isolation

Mitochondria were isolated as described previously (Yu *et al.*, 2014). Briefly, the cells were suspended in cold isolation buffer (10 mM Hepes pH 7.2, 1 mM EDTA, 320 mM sucrose) containing protease inhibitor and homogenized in a Dounce homogenizer. The homogenate was centrifuged at 700 × g for 8 min. The first supernatant was saved, and the pellet was homogenized and centrifuged again. The two supernatants were pooled and centrifuged together at 17,000 × g for 15 min to obtain the mitochondrial pellet.

Western blotting and immunofluorescence

Western blotting was performed with 1:1000 of the following primary antibodies (Yu *et al.*, 2014): mouse anti-Drp1 (BD Biosciences), rabbit anti- phospho-Drp1-Ser616 (Cell Signaling Technology), rabbit anti-Mfn1 (Santa Cruz Biotech), rabbit anti-Mfn2 (Cell Signaling Technology), mouse anti-OPA1 (BD Biosciences), rabbit anti-VDAC (Cell Signaling Technology), mouse anti-cytochrome c (Santa Cruz Biotech) and mouse anti-actin (Santa Cruz Biotech). Horseradish peroxidase-conjugated anti-rabbit and anti-mouse antibodies were used as secondary antibodies.

Indirect immunofluorescence was performed as described previously (Yu *et al.*, 2014). Briefly, cells cultured on coverslip were fixed in 4% paraformaldehyde and permeabilized with 0.1% Triton X-100. Mouse anti-Drp1 (BD Biosciences) antibody was used for primary antibody and Alexa 594-conjugated antibodies (Invitrogen) were used for the secondary antibody. Fluorescence images were acquired and adjusted by using ImageJ software (NIH Image).

Statistical analysis

Data are expressed as mean ± standard deviations. Statistical significance was established by t-test, or one- or two-way ANOVA followed by post test for comparisons. Comparisons of mitochondrial morphological parameters were carried out using nonparametric Mann–Whitney test.

Results

Heat acclimation improved cell viability during heat shock exposure and modified mitochondrial morphology in C2C12 myoblasts

Following treatment with HA, C2C12 myoblasts showed significantly higher survival rates during exposure to heat shock compared to control cells (Figure 1A). Morphological examination revealed that HA-treated myoblasts contained overly elongated mitochondrial networks, whereas control cells maintained predominantly tubular mitochondria (Figure 1B). Furthermore, expression of mitochondrial fission protein Drp1 was lower in the mitochondrial fractions from HA-treated cells compared to control cells (Figure 1C). We also performed western blot of VDAC and actin in whole cell lysate and found no differences in the ratio of VDAV to actin between control and HA cells (1.13 ± 0.05 versus 1.16 ± 0.04, $p > 0.05$). No changes in mitochondrial fusion proteins OPA1, and Mfn 1 and 2 were found in HA-treated cells (Figure 1D). Mitochondrial morphology and dynamics were further examined in the gastrocnemius muscles of control and HA-exposed mice. Transmission electron microscope (TEM) images revealed larger SS and IMF mitochondria in the muscles of HA-exposed mice, compared to control mice (Figure 2A). Further quantitative analysis of major mitochondrial shape parameters indicated an increase in size of SS and IMF mitochondria in the muscles of HA-exposed mice (Table 1 and Figure 2B). Finally, expression of Drp1 was lower in the mitochondrial fractions of the gastrocnemius muscles from HA-exposed mice compared to control mice (Figure 2C).

Exposure to heat shock caused apoptotic cell death

The survival rates of both C2C12 myoblast and myotubes decreased with duration of heat shock exposure in a similar manner: < 70% survived after exposure to heat shock for 4 hour (Figure 3A). We examined mitochondrial events, known to occur during programed cell death (apoptosis), in C2C12 myoblast following exposure to heat shock. Immunofluorescence staining and western blotting showed that cytochrome c was located inside mitochondria under normal incubation, but was released from mitochondria into the cytosol of C2C12 myoblasts during heat shock exposure (Figure 3B). Cell injury was further assessed by using Caspase 3/7 Green and Annexin V Apoptosis Detection kits. Heat shock-exposed caused C2C12 myoblasts became Caspase 3/7 (Figure 3C) and Annexin V positive (Figure 3D).

Exposure to heat shock caused mitochondrial fragmentation in C2C12 myoblasts

We examined mitochondrial morphology in C2C12 cells after exposure to heat shock. Mitochondria in C2C12 myotubes were small and densely packed, and very difficult to discern. C2C12 myoblasts contained more conventional tubular mitochondria under our experimental conditions and thus were used for mitochondrial morphology analysis. Mitochondria form filamentous and often interconnected networks under normal incubation at 37 °C, but the mitochondrial networks became mostly small and punctate units in C2C12 myoblasts after exposure to heat shock (Figure 4A). We conducted time course experiments and found that mitochondria rapidly became fragmented when exposed to heat shock (Figure 4B): the number of cells containing fragmented mitochondria increased from ~10% at 0 min to ~ 47% at 15 min and reached a plateau of ~ 91% at 30 min and thereafter.

Exposure to heat shock caused activation of mitochondrial fission in C2C12 myoblasts

Mitochondrial structural dynamics are regulated by the fusion and fission of the organelles with an increase in fission activity, which results in mitochondrial fragmentation. Therefore, we assessed mitochondrial fission protein Drp1. Whole cell lysate immunoblotting showed no significant changes in total Drp1 after exposure to heat shock (Figure 5A). We further

examined cytosolic and mitochondrial Drp1 levels in C2C12 cells after incubation at 43 °C for 0, 15, 30 and 60 min (Figure 5A). We found a time-dependent increase in the mitochondrial fractions of Drp1 and concurrent decrease in its cytosolic fractions. To verify heat-induced mitochondrial translocation of Drp1, we performed immunofluorescence image and intensity analysis of Drp1 and mitochondria in C2C12 cells (Figure 5B). Under normal incubation, Drp1 predominantly resided throughout the cytosol, with limited association with the tubular mitochondria. After exposure to heat shock, cytosol Drp1 decreased, whereas the majority of Drp1 puncta were co-localized with the fragmented mitochondria. Western blot analysis also showed significantly increased phosphorylation of Drp1 at serine-616 in heat shock-exposed C1C12 myoblasts (Figure 5C).

Inhibition of mitochondrial fission protected cell viability and mitochondrial structural integrity against heat shock

To determine whether resistance of cells to heat injury is mediated by mitochondrial dynamics, we tested the effects of inhibiting mitochondrial fission on cell viability by Mdivi-1 and Drp1 shRNA, which inhibits Drp1 assembly and GTPase activity (Cassidy-Stone *et al.*, 2008) and suppresses the transcription of Drp1 gene in infected cells, respectively. Pretreatment with Mdivi-1 or Drp1 shRNA significantly improved the survival rates of C2C12 myoblast during exposure to heat shock and significantly reduced the number of Annexin V positive apoptotic cells (Figure 6A). We found that Drp1 shRNA also prevented cytochrome c release and caspase activation in C2C12 myoblast during exposure to heat shock (Figure 6B).

Mitochondrial morphology analysis revealed a significant reduction in the number of fragmented mitochondria in C2C12 myoblast pretreated with Mdivi-1 or infected with Drp1 shRNA following heat shock exposure (Figure 6C). Only ~5.3% of Mdivi-1-treated cells contained fragmented mitochondria compared to ~82.5% of cells pretreated with vehicle. A similar reduction in mitochondrial fragmentation (> 93% cells maintained tubular mitochondrial networks) was found in cells infected with Drp1 shRNA. Western analysis showed that expression of Drp1 protein was reduced by ~80% in Drp1 shRNA-treated cells,

compared to cells infected with vehicle control, Lentiviral Particle carrying copGFP (Santa Cruz) (Figure 6D).

Inhibition of mitochondrial fission reduced loss of mitochondrial membrane potential and production of ROS in C2C12 myoblasts caused by heat shock

We measured mitochondrial membrane potential magnitude in C2C12 myoblasts labeled with MitoTracker Green and TMRE. Exposure to heat shock caused a significant decline of mitochondrial TMRE, not MitoTracker Green, fluorescence in C2C12 myoblasts (Figure 7A). Time-lapse experiments further revealed that the decrease in mitochondrial TMRE fluorescence occurred as early as ~ 20-25 min (Figure 7B). Pretreatment with Mdivi-1 or Drp1 shRNA prevented heat shock-induced loss of mitochondrial membrane potential in C2C12 cells (Figure 7C).

Exposing C2C12 myoblasts to heat shock caused a time-dependent increase in DHE fluorescence, an indicator of ROS (Figure 7D). The fluorescence signal increased from baseline to ~2 fold at 1 hour and ~5 fold at 4 hours of exposure to heat shock. Pretreatment with Mdivi-1 or Drp1 shRNA prevented an increase in ROS in C2C12 cells induced by heat shock.

Exposure to heat shock caused OPA1 cleavage and loss of mitochondrial membrane potential in C2C12 myoblasts in a time-dependent manner

We examined mitochondrial fusion proteins in C2C12 myoblasts exposed heat shock. No significant changes in Mfn1 and Mfn2 levels were found in C2C12 cells following up to 60 minutes of heat shock exposure (Figure 8A). Western blot analysis of whole cell lysates with an OPA1 antibody (BD Biosciences) revealed at least one long and one short form of OPA1 in C2C12 cells before exposure to heat shock (Figure 8B). No changes in OPA1 levels were detected in cells 15 minutes into heat exposure. The long form of OPA1 significantly decreased and a new short form band appeared, which indicates cleavage of high molecular weight forms of OPA1 at 30 min into heat exposure.

Discussion

Fusion-fission dynamics adapt the morphology of the mitochondrial compartment to various metabolic needs of cells and enable them to regain homeostasis and survive under many stress conditions. The present study showed that HA and heat shock affects mitochondrial morphology in C2C12 cells primarily by reducing and increasing recruitment of the fission mediator Drp1 to mitochondria. Our results demonstrate key mitochondrial events involved in the HA and heat shock responses and provide evidence supporting a new mechanism - Drp1-mediated mitochondrial fission - underlying the susceptibility of muscle cells to heat-induced injury.

Mitochondria typically form a reticular network radiating from the nucleus to create an interconnected system for ensuring essential energy supplies to the cell; they are able to adapt to environmental challenges by remodeling their morphology. The formation of elongated mitochondrial networks is a conserved mechanism engaged during chronic cellular stress (e.g., nutrient deprivation) as a means to maintain ATP production, avoid mitophagy, and improve tolerance of mtDNA mutations by diluting damaged mitochondrial contents across the mitochondrial network (Tondera *et al.*, 2009; Rambold *et al.*, 2011; Mishra *et al.*, 2015; Senyilmaz *et al.*, 2015). On the other hand, fragmented mitochondria are associated with various pathological conditions (Yoon *et al.*, 2011; Galluzzi *et al.*, 2012; Hoppins & Nunnari, 2012; Youle & van der Bliek, 2012; Archer, 2013). In the present study, we expanded previous findings by showing that HA-exposed mouse skeletal muscle tissue and cells shared a common feature of elongated mitochondria: HA resulted in increased resistance against heat shock-induced injury in muscle cells. Mitochondrial networks are maintained through the complex coordination of fission and fusion regulated by a number of key mitochondrial morphology proteins. Our results indicate that HA-induced mitochondrial morphological remodeling is due to an imbalance favoring fusion over fission, which is caused by down-regulation of Drp1. The mechanisms behind these changes remain unclear. We are not aware of any studies linking HA to cellular energy stress, but HA may likely have an indirect effect on mitochondrial morphology. For instance, HA is known to cause an adaptation response with up-regulation of HSF1 and HSP70s (Tetievsky *et al.*, 2008). Expression of HSP72 is critical in promoting mitochondrial fusion in skeletal muscle (Drew

et al., 2014). A single bout of one-hour mild heat exposure (40 °C) is reportedly sufficient to cause up-regulation of HSP72 in C2C12 cells (Liu & Brooks, 2012). In the present study, HA-treated cells likely had upregulated HSP72, which helped maintain mitochondrial homeostasis and morphology during heat shock exposure.

Although fused or elongated mitochondrial networks help cells survive starvation, it is unknown whether this morphological adaptation in mitochondria is associated with resistance of cells against heat insults. The present study suggests that elongation of mitochondria with decreased fission may be advantageous under lethal heat conditions. We showed that heat shock caused mitochondrial fragmentation and Drp1 translocation in control but not in HA-treated muscle cells. The homeostatic alterations in mitochondrial fission and morphology in HA-treated cells may limit recruitment of Drp1 and resist mitochondrial breakdown under heat stress. In addition, as discussed above, HA is known to cause overexpression of heat stress proteins. HSP70 can inhibit stress protein kinases (Gabai *et al.*, 1997) that activate Drp1 under mitochondrial stress (Kashatus *et al.*, 2015; Park *et al.*, 2015). Thus, through complex mechanisms, HA may alter mitochondrial morphology and dynamics to protect cells against mitochondria-dependent apoptosis during heat exposure.

Our results provide evidence that cells exposed to lethal heat shock undergo apoptotic death. Limited information is available on how heat stress initiates apoptosis signaling. Apoptotic cell death is initiated and activated by diverse internal or external pro-apoptotic insults. Depending on the type of stimulus, the apoptotic signaling cascades undergo a mitochondrial-dependent, ligand-mediated death receptor, or an endoplasmic reticulum stress-induced pathway (Adams, 2003). The execution phase of apoptosis usually involves activation of a family of protease proteins called caspases. Heat-induced apoptosis of C2C12 cells is likely activated primarily through an intrinsic, mitochondria-dependent pathway. Several events, including mitochondrial oxidative stress, observed in cells exposed to heat shock are linked to activation of caspases, which likely serve as the primary mediators of apoptosis (Primeau *et al.*, 2002; Palmer *et al.*, 2011; Rigoulet *et al.*, 2011). These cellular events ultimately lead to changes in the integrity of the mitochondrial membrane (Westphal *et al.*, 2011). Loss of mitochondrial integrity results in release of pro-apoptotic proteins, including cytochrome c, which facilitate recruitment of caspases to form the apoptosome.

This downstream caspase activation results in subsequent apoptotic cell death under heat conditions (Katschinski *et al.*, 2000; Wang *et al.*, 2013). Thus, several primary pro-apoptotic factors clearly contributed to initiation and activation of heat-induced apoptosis of C2C12 cells.

In the present study, we demonstrated that HA improved viability of C2C12 cells against heat. Reduced mitochondrial Drp1 and increased mitochondrial size were found in both C2C12 cells and mouse gastrocnemius muscles following HA. Whether these changes directly contributed to HA-induced heat tolerance of cells remains unclear. Mitochondrial apoptotic susceptibility to heat stress is likely dependent upon the ratio of pro- and anti-apoptotic Bcl-2 family proteins, including pro-apoptotic Bax and anti-apoptotic Bcl-2 (Primeau *et al.*, 2002). Further investigation of HA effects on Bcl-2 family proteins should provide information about improved ability of HA-treated cells to survive subsequent heat stress. Mitochondrial fission is involved in skeletal muscle differentiation and growth. Inhibition of mitochondrial fission has been shown to impair myogenesis (Kim *et al.*, 2013), whereas severe burn injury has been shown to induce skeletal muscle regeneration (Fry *et al.*, 2016). Whether heat shock would stimulate and HA would inhibit muscle regeneration process has yet to be examined.

Our results revealed proteolytic conversion of larger into smaller isoforms of OPA1 in C2C12 cells during heat exposure. Whether this was caused directly by heat or indirectly by other mitochondrial events remains unclear. It is known that OPA1 plays a critical role in maintaining mitochondrial inner membrane integrity (Lee & Yoon, 2014). Disruption of OPA1 assembly can cause an increase of mitochondrial permeability (Frezza *et al.*, 2006; Yamaguchi *et al.*, 2008) and dissipation of mitochondrial membrane potential (Lee & Yoon, 2014). On the other hand, loss of mitochondrial membrane potential may also lead to the cleavage of OPA1 and fusion inhibition (Duvezin-Caubet *et al.*, 2006; Ishihara *et al.*, 2006; Liu *et al.*, 2009). The fact that mitochondrial membrane potential (Figure 7A) in C2C12 cells declined well before, not concurrently with, proteolysis of OPA1 (Figure 8B) during heat exposure seems to negate a direct link between them. Instead, Drp1-dependent mitochondrial fission (Figure 4B) preceded all the mitochondrial events, including release of ROS, loss of membrane potential and cleavage of OPA1 during heat exposure (Figures 7A, 7D and 8B).

Overall, our data support Drp1 over OPA1 as the primary mediator involved in the regulation of cell susceptibility to heat-induced apoptosis. First, translocation and phosphorylation of Drp1 and mitochondrial fragmentation preceded the cleavage of OPA1, and second, HA affected expression of Drp1, but not OPA1 in muscle cells and tissues. However, factors that may act as an upstream Drp1 signal in heat stress have yet to be determined.

In conclusion, the findings of the present study provide novel insights into the role of mitochondria in the regulation of heat-induced apoptosis of muscle cells. Our results demonstrate that HA and heat shock cause changes in mitochondrial morphology of muscle cells by acting on Drp1, which results in favoring mitochondrial fusion and fission respectively. Inhibition of Drp1-dependent mitochondrial division improves mitochondrial morphology and cell viability during heat exposure. Thus, we propose that Drp1 may serve as a biomarker for susceptibility to heat stress and a candidate for preventing heat injury.

Additional information

Competing interests

The authors declare that there are no competing interests.

Author contributions

T.Y. designed and performed the experiments, analyzed the data and helped prepare the manuscript. P.D. provided editorial advice. Y.C. developed the concept and project, analyzed the data and wrote the manuscript.

Funding

This work was supported by Congressionally Directed Medical Research Program Award W81XWH-14-2-0133.

References

Abdelnasir A, Sun JR, Cheng YF, Chen HB, Tang S, Kemper N, Hartung J & Bao ED. (2014). Evaluation of Hsp47 expression in heat-stressed rat myocardial cells in vitro and in vivo. *Genet Mol Res* **13,** 10787-10802.

Adams JM. (2003). Ways of dying: multiple pathways to apoptosis. *Genes Dev* **17,** 2481-2495.

Archer SL. (2013). Mitochondrial dynamics--mitochondrial fission and fusion in human diseases. *N Engl J Med* **369,** 2236-2251.

Block BA. (1994). Thermogenesis in muscle. *Annu Rev Physiol* **56,** 535-577.

Cassidy-Stone A, Chipuk JE, Ingerman E, Song C, Yoo C, Kuwana T, Kurth MJ, Shaw JT, Hinshaw JE, Green DR & Nunnari J. (2008). Chemical inhibition of the mitochondrial division dynamin reveals its role in Bax/Bak-dependent mitochondrial outer membrane permeabilization. *Dev Cell* **14,** 193-204.

Chung J, Nguyen AK, Henstridge DC, Holmes AG, Chan MH, Mesa JL, Lancaster GI, Southgate RJ, Bruce CR, Duffy SJ, Horvath I, Mestril R, Watt MJ, Hooper PL, Kingwell BA, Vigh L, Hevener A & Febbraio MA. (2008). HSP72 protects against obesity-induced insulin resistance. *Proceedings of the National Academy of Sciences of the United States of America* **105,** 1739-1744.

Drew BG, Ribas V, Le JA, Henstridge DC, Phun J, Zhou Z, Soleymani T, Daraei P, Sitz D, Vergnes L, Wanagat J, Reue K, Febbraio MA & Hevener AL. (2014). HSP72 is a mitochondrial stress sensor critical for Parkin action, oxidative metabolism, and insulin sensitivity in skeletal muscle. *Diabetes* **63,** 1488-1505.

Drust B, Rasmussen P, Mohr M, Nielsen B & Nybo L. (2005). Elevations in core and muscle temperature impairs repeated sprint performance. *Acta physiologica Scandinavica* **183,** 181-190.

Duvezin-Caubet S, Jagasia R, Wagener J, Hofmann S, Trifunovic A, Hansson A, Chomyn A, Bauer MF, Attardi G, Larsson NG, Neupert W & Reichert AS. (2006). Proteolytic processing of OPA1 links mitochondrial dysfunction to alterations in mitochondrial morphology. *J Biol Chem* **281,** 37972-37979.

Ferri KF & Kroemer G. (2001). Organelle-specific initiation of cell death pathways. *Nat Cell Biol* **3,** E255-263.

Frezza C, Cipolat S, Martins de Brito O, Micaroni M, Beznoussenko GV, Rudka T, Bartoli D, Polishuck RS, Danial NN, De Strooper B & Scorrano L. (2006). OPA1 controls apoptotic cristae remodeling independently from mitochondrial fusion. *Cell* **126,** 177-189.

Fry CS, Porter C, Sidossis LS, Nieten C, Reidy PT, Hundeshagen G, Mlcak R, Rasmussen BB, Lee JO, Suman OE, Herndon DN & Finnerty CC. (2016). Satellite cell activation and apoptosis in skeletal muscle from severely burned children. *The Journal of physiology*.

Gabai VL, Meriin AB, Mosser DD, Caron AW, Rits S, Shifrin VI & Sherman MY. (1997). Hsp70 prevents activation of stress kinases. A novel pathway of cellular thermotolerance. *The Journal of biological chemistry* **272,** 18033-18037.

Galluzzi L, Kepp O, Trojel-Hansen C & Kroemer G. (2012). Mitochondrial control of cellular life, stress, and death. *Circ Res* **111,** 1198-1207.

Gupte AA, Bomhoff GL, Swerdlow RH & Geiger PC. (2009). Heat treatment improves glucose tolerance and prevents skeletal muscle insulin resistance in rats fed a high-fat diet. *Diabetes* **58,** 567-578.

Hoppins S & Nunnari J. (2012). Cell Biology. Mitochondrial dynamics and apoptosis--the ER connection. *Science* **337,** 1052-1054.

Horowitz M, Umschweif G, Yacobi A & Shohami E. (2015). Molecular programs induced by heat acclimation confer neuroprotection against TBI and hypoxic insults via cross-tolerance mechanisms. *Front Neurosci* **9,** 256.

Ishihara N, Fujita Y, Oka T & Mihara K. (2006). Regulation of mitochondrial morphology through proteolytic cleavage of OPA1. *EMBO J* **25,** 2966-2977.

Islam A, Lv YJ, Abdelnasir A, Rehana B, Liu ZJ, Zhang M, Tang S, Cheng YF, Chen HB, Hartung J & Bao ED. (2013). The role of Hsp90alpha in heat-induced apoptosis and cell damage in primary myocardial cell cultures of neonatal rats. *Genet Mol Res* **12,** 6080-6091.

Kashatus JA, Nascimento A, Myers LJ, Sher A, Byrne FL, Hoehn KL, Counter CM & Kashatus DF. (2015). Erk2 phosphorylation of Drp1 promotes mitochondrial fission and MAPK-driven tumor growth. *Mol Cell* **57,** 537-551.

Katschinski DM, Boos K, Schindler SG & Fandrey J. (2000). Pivotal role of reactive oxygen species as intracellular mediators of hyperthermia-induced apoptosis. *J Biol Chem* **275,** 21094-21098.

Kim B, Kim JS, Yoon Y, Santiago MC, Brown MD & Park JY. (2013). Inhibition of Drp1-dependent mitochondrial division impairs myogenic differentiation. *American journal of physiology Regulatory, integrative and comparative physiology* **305,** R927-938.

Lee H & Yoon Y. (2014). Transient contraction of mitochondria induces depolarization through the inner membrane dynamin OPA1 protein. *J Biol Chem* **289,** 11862-11872.

Liu CT & Brooks GA. (2012). Mild heat stress induces mitochondrial biogenesis in C2C12 myotubes. *J Appl Physiol (1985)* **112,** 354-361.

Liu X, Weaver D, Shirihai O & Hajnoczky G. (2009). Mitochondrial 'kiss-and-run': interplay between mitochondrial motility and fusion-fission dynamics. *EMBO J* **28,** 3074-3089.

Mishra P, Varuzhanyan G, Pham AH & Chan DC. (2015). Mitochondrial Dynamics is a Distinguishing Feature of Skeletal Muscle Fiber Types and Regulates Organellar Compartmentalization. *Cell Metab* **22,** 1033-1044.

Monastyrskaya EA, Andreeva LV, Duchen MR, Manukhina EB & Malyshev IY. (2003). Direct and cross-protective effects of heat adaptation in cultured cells. *Bull Exp Biol Med* **135,** 127-129.

Palmer CS, Osellame LD, Stojanovski D & Ryan MT. (2011). The regulation of mitochondrial morphology: intricate mechanisms and dynamic machinery. *Cell Signal* **23,** 1534-1545.

Park JH, Ko J, Hwang J & Koh HC. (2015). Dynamin-related protein 1 mediates mitochondria-dependent apoptosis in chlorpyrifos-treated SH-SY5Y cells. *Neurotoxicology* **51,** 145-157.

Picard M, White K & Turnbull DM. (2013). Mitochondrial morphology, topology, and membrane interactions in skeletal muscle: a quantitative three-dimensional electron microscopy study. *Journal of applied physiology* **114,** 161-171.

Primeau AJ, Adhihetty PJ & Hood DA. (2002). Apoptosis in heart and skeletal muscle. *Can J Appl Physiol* **27,** 349-395.

Qian L, Song X, Ren H, Gong J & Cheng S. (2004). Mitochondrial mechanism of heat stress-induced injury in rat cardiomyocyte. *Cell Stress Chaperones* **9,** 281-293.

Rambold AS, Kostelecky B, Elia N & Lippincott-Schwartz J. (2011). Tubular network formation protects mitochondria from autophagosomal degradation during nutrient starvation. *Proc Natl Acad Sci U S A* **108,** 10190-10195.

Rigoulet M, Yoboue ED & Devin A. (2011). Mitochondrial ROS generation and its regulation: mechanisms involved in H(2)O(2) signaling. *Antioxid Redox Signal* **14,** 459-468.

Sanjuan Szklarz LK & Scorrano L. (2012). The antiapoptotic OPA1/Parl couple participates in mitochondrial adaptation to heat shock. *Biochim Biophys Acta* **1817,** 1886-1893.

Senyilmaz D, Virtue S, Xu X, Tan CY, Griffin JL, Miller AK, Vidal-Puig A & Teleman AA. (2015). Regulation of mitochondrial morphology and function by stearoylation of TFR1. *Nature* **525,** 124-128.

Taylor LE, Kronfeld DS, Ferrante PL, Wilson JA & Tiegs W. (1998). Blood-gas measurements adjusted for temperature at three sites during incremental exercise in the horse. *Journal of applied physiology* **85,** 1030-1036.

Tetievsky A, Cohen O, Eli-Berchoer L, Gerstenblith G, Stern MD, Wapinski I, Friedman N & Horowitz M. (2008). Physiological and molecular evidence of heat acclimation memory: a lesson from thermal responses and ischemic cross-tolerance in the heart. *Physiol Genomics* **34,** 78-87.

Tondera D, Grandemange S, Jourdain A, Karbowski M, Mattenberger Y, Herzig S, Da Cruz S, Clerc P, Raschke I, Merkwirth C, Ehses S, Krause F, Chan DC, Alexander C, Bauer C, Youle R, Langer T & Martinou JC. (2009). SLP-2 is required for stress-induced mitochondrial hyperfusion. *EMBO J* **28,** 1589-1600.

Wang Z, Cai F, Chen X, Luo M, Hu L & Lu Y. (2013). The role of mitochondria-derived reactive oxygen species in hyperthermia-induced platelet apoptosis. *PLoS One* **8,** e75044.

Westphal D, Dewson G, Czabotar PE & Kluck RM. (2011). Molecular biology of Bax and Bak activation and action. *Biochim Biophys Acta* **1813,** 521-531.

Yamaguchi R, Lartigue L, Perkins G, Scott RT, Dixit A, Kushnareva Y, Kuwana T, Ellisman MH & Newmeyer DD. (2008). Opa1-mediated cristae opening is Bax/Bak and BH3 dependent, required for apoptosis, and independent of Bak oligomerization. *Mol Cell* **31,** 557-569.

Yoon Y, Galloway CA, Jhun BS & Yu T. (2011). Mitochondrial dynamics in diabetes. *Antioxid Redox Signal* **14,** 439-457.

Youle RJ & van der Bliek AM. (2012). Mitochondrial fission, fusion, and stress. *Science* **337,** 1062-1065.

Yu T, Wang L, Lee H, O'Brien DK, Bronk SF, Gores GJ & Yoon Y. (2014). Decreasing mitochondrial fission prevents cholestatic liver injury. *The Journal of biological chemistry* **289,** 34074-34088.

Table 1. Morphological parameters for SS and IMF mitochondria in the gastrocnemius muscles of control and HA mice

		Median	Mean (SD)	Min	Max	Skewness
SS						
Surface area, μm^2	control	0.18	0.24 (0.21)	0.04	1.19	1.61
	HA	0.39*	0.44 (0.26)	0.10	1.54	1.76
Perimeter, μm	control	1.89	2.32 (1.33)	0.92	9.32	2.00
	HA	3.08*	3.25 (1.28)	1.27	9.32	1.77
Circularity (0-1)	control	0.56	0.56 (0.14)	0.20	1	0.20
	HA	0.54	0.55 (0.15)	0.21	1	0.22
Feret's diameter, μm	control	0.70	0.92 (0.52)	0.33	3.30	1.49
	HA	1.17*	1.25 (0.48)	0.44	3.30	1.41
Form factor	control	1.78	1.91 (0.55)	1.00	4.98	1.45
	HA	1.85	1.98 (0.62)	1.00	4.76	1.18
Aspect ratio	control	2.66	2.86 (1.10)	1.02	6.20	0.87
	HA	2.45*	2.67 (1.17)	1.02	7.78	1.52
IMF						
Surface area, μm^2	control	0.06	0.07 (0.05)	0.02	0.41	2.99
	HA	0.18*	0.25 (0.22)	0.04	1.23	1.77
Perimeter, μm	control	1.14	1.21 (0.36)	0.58	3.39	2.10
	HA	1.89*	2.32 (1.34)	0.92	9.32	2.00
Circularity (0-1)	control	0.61	0.60 (0.12)	0.28	1	0.20
	HA	0.56*	0.56 (0.14)	0.20	1	0.20
Feret's diameter, μm	control	0.44	0.47 (0.15)	0.22	1.29	1.91
	HA	0.70*	0.92 (0.53)	0.33	3.30	1.49
Form factor	control	1.65	1.73 (0.36)	1.00	3.61	1.11
	HA	1.78*	1.91 (0.55)	1.00	4.98	1.45
Aspect ratio	control	2.40	2.54 (0.81)	1.02	5.80	0.75
	HA	2.57	2.80 (1.11)	1.02	6.20	0.96

* $p < 0.01$ versus control by nonparametric Mann–Whitney test. n = 200 SS and 200 IMF mitochondria for each of control and HA groups.

Figure 1. Heat acclimation (HA) improves cell viability during heat shock exposure and affects mitochondrial morphology and Drp1 in C2C12 myoblasts. (**A**) Viability of control and HA-treated C2C12 cells during incubation at 43 °C. Control cells were maintained at 37 °C all the time for three days, whereas HA-treated cells were incubated at 39.5 °C for 3 hours per day (at 37 °C all other times) for three days. Data were obtained from 3 experiments; * $p < 0.01$ versus control by two-way ANOVA/Bonferroni post-test. (**B**) Representative immunofluorescence images of mitochondria (green) and Drp1 distribution (red), and percentages of cells with elongated mitochondria in control and HA-treated C2C12 cells following a 4 hour incubation at 43 °C. Data were obtained from 3 independent experiments and ~300 cells were counted. DAPI: blue fluorescent DNA dye; scale bar 5 μm. (**C**) Western blot analysis of Drp1 in mitochondrial fractions from C2C12 cells following 3 days heat acclimation. Experiments were repeated at least 3 times. *$p < 0.001$ versus control. (**D**) Representative western blot of OPA1, Mfn1, and Mfn2 in control and HA-treated C2C12 cells.

Figure 2. Heat acclimation (HA) causes morphological changes in mitochondria and reduces Drp1 in mitochondrial fraction of mouse gastrocnemius muscles. (**A**) Representative transmission electron microscopy images of subsarcolemmal (SS) and intermyofibrillar (IMF) mitochondria in the gastrocnemius muscles of control and HA mice. Scale bar: 5 μm. **(B)** Histographic representation of morphological parameters for SS and IMF mitochondria in the gastrocnemius muscles of control and HA mice. n = 200 SS and 200 IMF mitochondria. (**C**) Western blot analysis of Drp1 in mitochondrial fractions from the gastrocnemius muscles of control and HA mice. HA mice were exposed to 33 °C in an environmental chamber for 3 hours/day (at 21 °C all other times) for 10 consecutive days; control mice were maintained at 21 °C for 10 consecutive days. *$p < 0.001$ versus control, n = 3 per group.

Figure 3. Heat shock exposure induces apoptotic cell death. (**A**) Viability of C2C12 myoblasts and myotubes during incubation at 43 °C. Cell viability was measured by trypan blue exclusion assay. Data were obtained from 3 experiments; *$p < 0.01$ versus 0 hour by one-way ANOVA with Dunnett's post test. (**B**) Representative immunofluorescence images of cytochrome c (red) and cytosolic expression of cytochrome c in C2C12 myoblasts

following a 4 hour incubation at 37 °C and 43 °C. DAPI: blue fluorescent DNA dye; Scale bar: 5 μm. (**C**) Representative fluorescence images and quantitative analysis of caspase-3/7 activities in C2C12 myoblasts following a 4 hour incubation at 37 °C and 43 °C. Experiments were repeated at least 3 times; *$p < 0.01$ versus 37 °C. Scale bar: 2 μm. (**D**) Representative fluorescence images of Annexin V in C2C12 myoblasts and quantitative analysis of Annexin V positive C2C12 myoblasts and myotubes following a 4 hour incubation at 37 °C and 43 °C. Experiments were repeated at least 3 times and data were obtained from 10 observation fields for each group; *$p < 0.001$ versus 37 °C. Scale bar: 5 μm.

Figure 4. Heat shock exposure causes mitochondrial fragmentation in C2C12 myoblasts. (**A**) Representative fluorescence images showing mitochondria morphology (red) in C2C12 myoblasts following a 30 minute incubation at 37 °C and 43 °C. Inserted windows, higher magnification of indicated area. DAPI: blue fluorescent DNA dye; scale bar: 5 μm. (**B**) Percent of C2C12 myoblasts with tubular and fragmented mitochondria following a 15-120 minute incubation at 43 °C. Experiments were repeated at least 3 times and ~300 cells were counted per experiment. * $p < 0.001$ versus Tubular; # $p < 0.001$ versus 0 minute by two-way ANOVA with Bonferroni post test.

Figure 5. Heat shock exposure induces mitochondrial translocation and phosphorylation of Drp1 in C2C12 myoblasts. Western blot analysis of Drp1 in whole cell lysates (total) and in mitochondrial (mito) and cytosol (cyto) fractions from C2C12 myoblasts during a 60 minute incubation at 43 °C. * $p < 0.01$ versus 37 °C by one-way ANOVA with Tukey's post trest. (**B**) Immunofluorescence images (left) and intensity profiles (right) of Drp1 (red) and mitochondria (green) in C2C12 myoblasts following a 30 minute incubation at 37 °C and 43 °C. Immunofluorescence intensities along the arrows were calculated and plotted (Drp1 in red and mitochondria in green) against the corresponding distances (pixels) of the arrows (right). N: nucleus. Scale bar: 2 μm. (**C**) Western blot analysis of Drp1 phosphorylation at Ser616 in C2C12 myoblasts during a 60 minute incubation at 43 °C. * $p < 0.001$ versus 37 °C, # $p < 0.01$ versus 15 or 30 min by one-way ANOVA with Tukey's post trest.

Figure 6. Inhibition of mitochondrial fission protects cell viability and mitochondrial morphology during heat shock exposure. (**A**) Cell viability of C2C12 myoblasts during incubation at 43 °C and quantitative analysis of Annexin V positive cells following a 4 hour incubation at 43 °C. Cells were labeled with Annexin V Apoptosis Detection kit and were pretreated with vehicle or Mdivi-1 or infected with Drp1 shRNA. Data were obtained from 10 observation fields for each group; * $p < 0.01$, shRNA versus vehicle; # $p < 0.01$, Mdivi-1versus vehicle by two-way ANOVA with Bonferroni post test for cell viability. * $p < 0.001$ versus vehicle for Annexin V by one-way ANOVA with Dunnett's post test. (**B**) Effects of Drp1 shRNA on cytosolic cytochrome c (cyt c) and caspase 3/7 activity in C2C12 myoblasts following a 4 hour incubation at 43 °C. C2C12 myoblasts were infected with vehicle (veh) or Drp1 shRNA before exposed to 43 °C. (**C**) Representative images of mitochondrial morphology in C2C12 myoblasts and quantitative analysis of C2C12 myoblasts with fragmented mitochondria following 30 minute incubation at 43 °C. Cells were pretreated with vehicle or Mdivi-1 or infected with Drp1 shRNA. Data were obtained from 3 experiments and ~300 cells were counted; * $p < 0.001$ versus vehicle by one-way ANOVA with Dunnett's post test. Scale bar: 5 μm. (**D**) Representative western blot of Drp1 in C2C12 myoblasts pretreated with vehicle or GFP or infected with Drp1 shRNA.

Figure 7. Inhibition of mitochondrial fission reduces loss of mitochondrial membrane potential and production of ROS in C2C12 myoblasts during heat shock exposure. (A) Representative images and quantitative analysis of MitoTracker Green (mito) and TMRE fluorescence in C2C12 myoblasts following a 30 minute incubation at 37 °C and 43 °C. Cells were stained with MitoTracker Green FM and TMRE, which accumulate in mitochondria based on mass and proton electrochemical gradient respectively. MitoTracker and TMRE fluorescence signals were acquired simultaneously. **(B)** Real time measurements of TMRM fluorescence intensity in C2C12 cells during incubation at 37 °C and 43 °C. n = 9. The validity of TMRM as an indicator of mitochondrial membrane potential was verified by using a mitochondria uncoupler, carbonyl cyanide 4-trifluoro-methoxyphenylhydrazone (FCCP, 2 μM). (**C**) Quantitative analysis of TMRE fluorescence as a function of incubation time at 43 °C. Cells were pretreated with vehicle or Mdivi-1 or infected with Drp1 shRNA. n = 30; * $p < 0.01$ versus 37 °C by one-way ANOVA with Dunnett's post test. (**D**) Representative DHE fluorescence images of C2C12 myoblasts following incubation at 43 °C

for 4 hours and quantitative analysis of DHE fluorescence as a function of incubation time at 43 °C. Cells were pretreated with vehicle or Mdivi-1 or infected with Drp1 shRNA. n = 30; * $p < 0.01$, shRNA versus vehicle; # $p < 0.01$, Mdivi-1 versus vehicle by two-way ANOVA with Bonferroni post test.

Figure 8. Heat shock exposure causes OPA1 cleavage and concurrent loss of mitochondrial membrane potential in C2C12 myoblasts. (**A**) Representative western blot of mitochondrial outer membrane fusion proteins, Mfn1 and Mfn2, in C2C12 cells following incubation at 43 °C for 0 to 60 minutes. (**B**) Representative western blot of short (S) and long (L) forms of mitochondrial inner membrane protein OPA1 in C2C12 cells following incubation at 43 °C for 0 to 60 minutes.

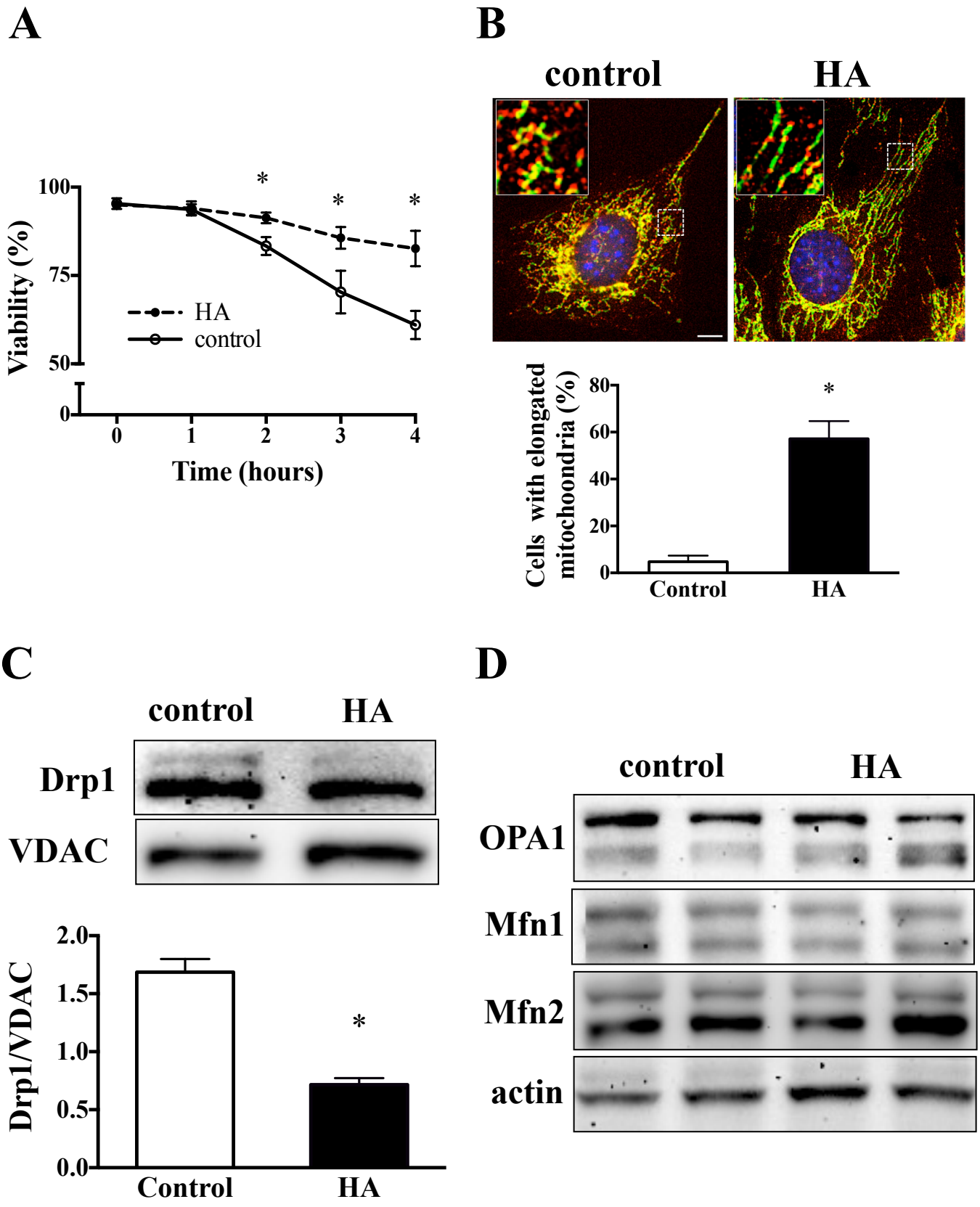
A
100
75
50
0
Viability (%)
HA
control
*
*
*
0
1
2
3
4
Time (hours)
B
control
HA
Cells with elongated mitochoondria (%)
80
60
40
20
0
*
Control
HA
C
control
HA
Drp1
VDAC
Drp1/VDAC
2.0
1.5
1.0
0.5
0.0
*
Control
HA
D
control
HA
OPA1
Mfn1
Mfn2
actin

Figure 1

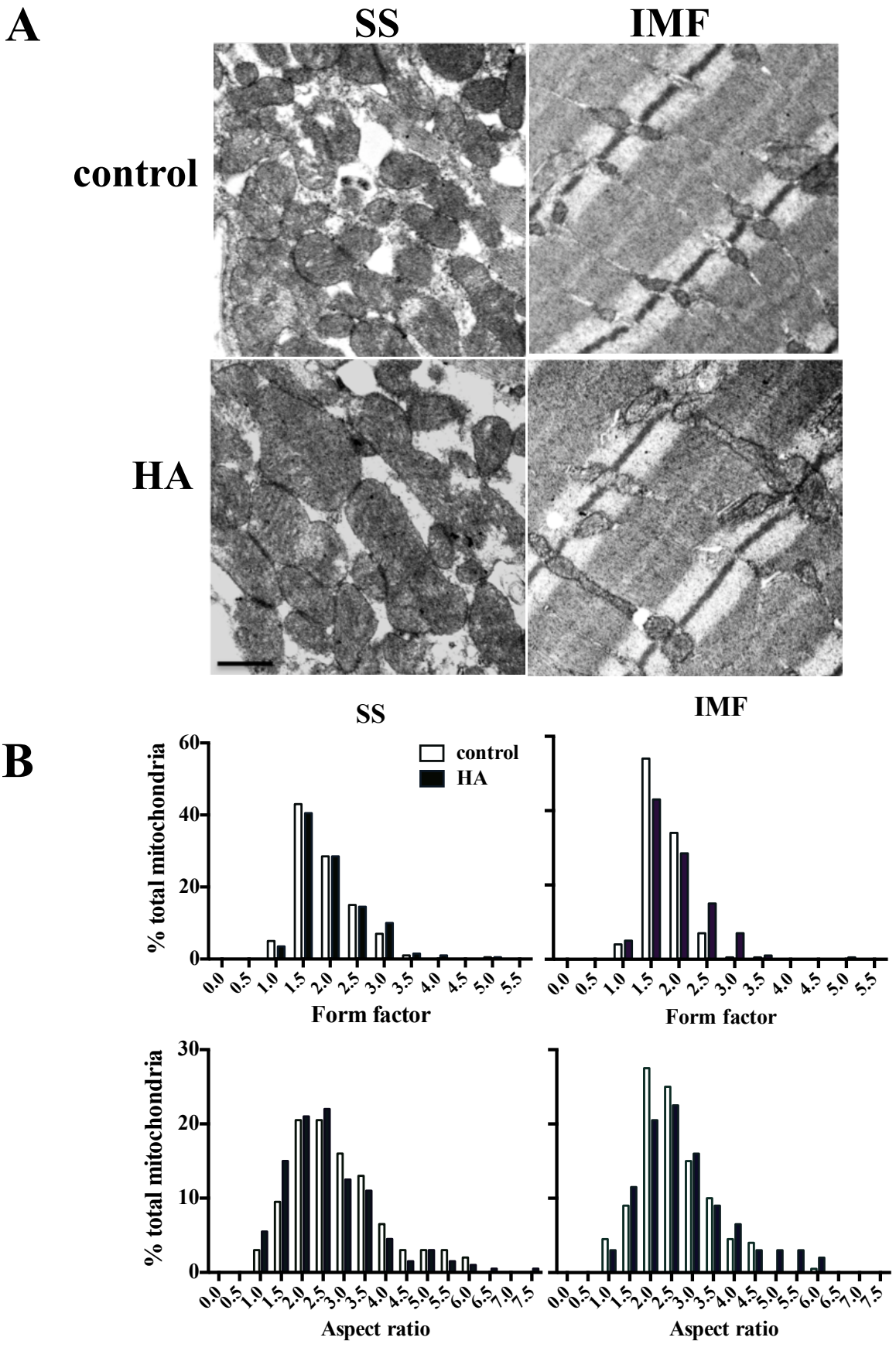
A
SS
IMF
control
HA
B
SS
IMF
control
HA
% total mitochondria
Form factor
Aspect ratio

Figure 2

C

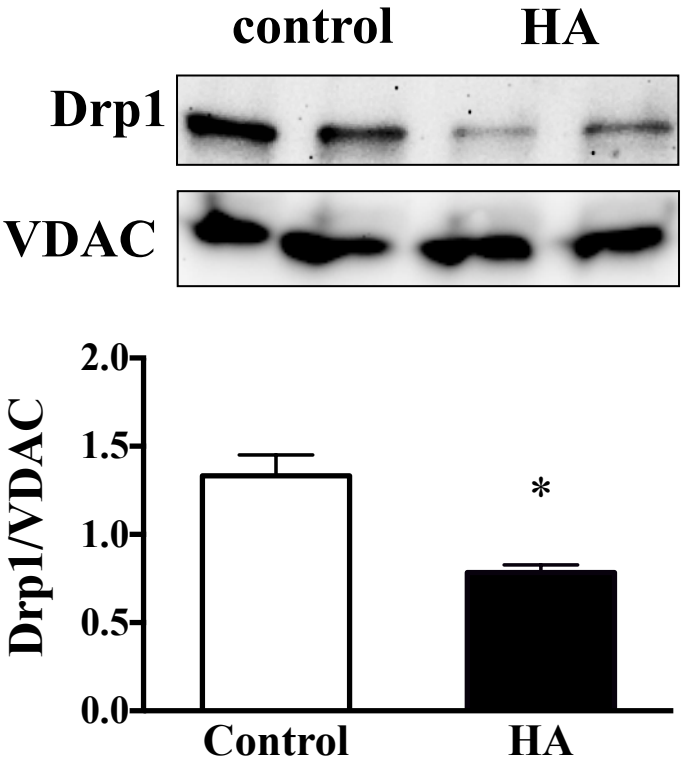

Figure 2

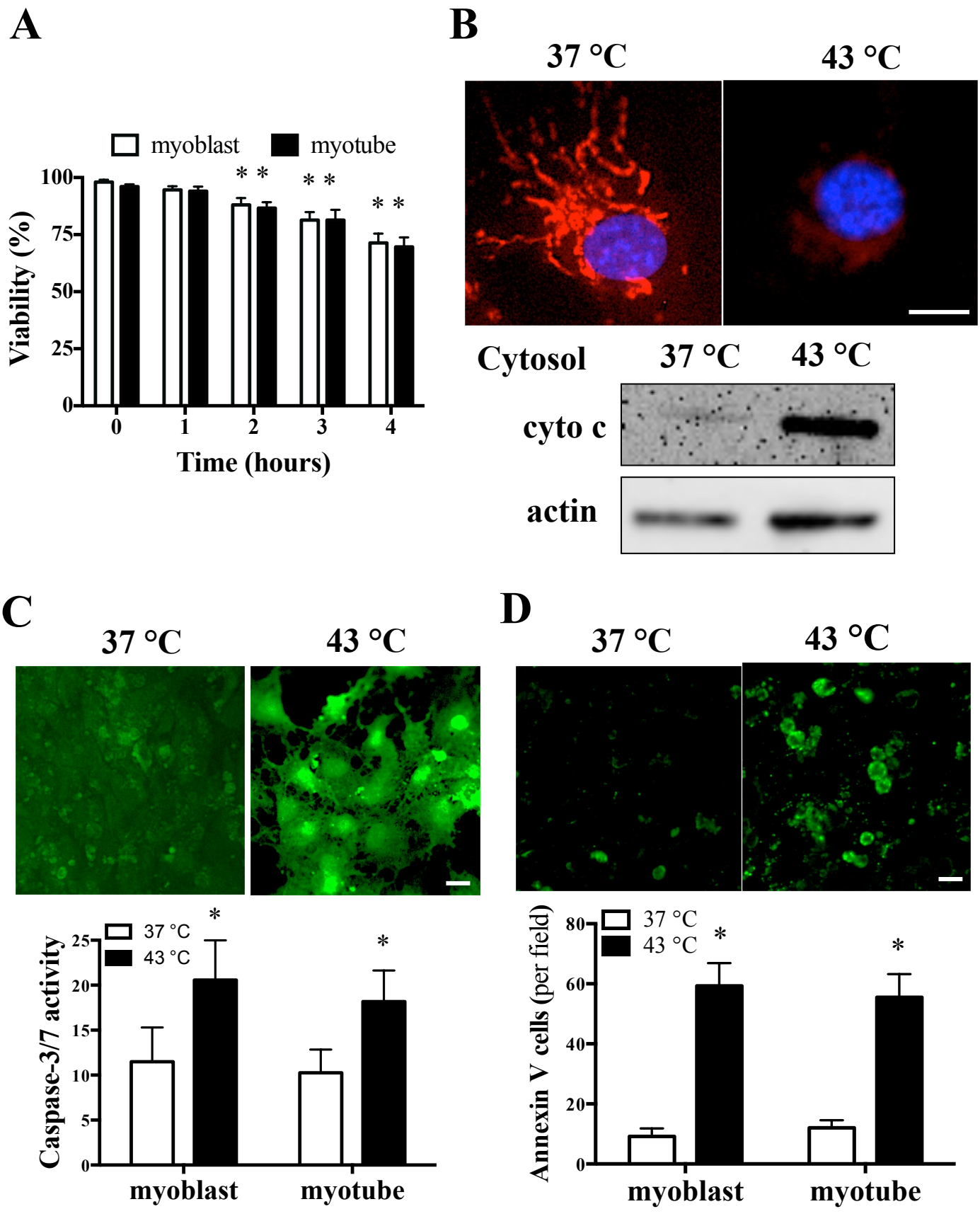
A
myoblast
myotube
Viability (%)
100
75
50
25
0
0
1
2
3
4
Time (hours)
B
37 °C
43 °C
Cytosol
37 °C
43 °C
cyto c
actin
C
37 °C
43 °C
Caspase-3/7 activity
37 °C
43 °C
myoblast
myotube
D
37 °C
43 °C
Annexin V cells (per field)
37 °C
43 °C
myoblast
myotube

Figure 3

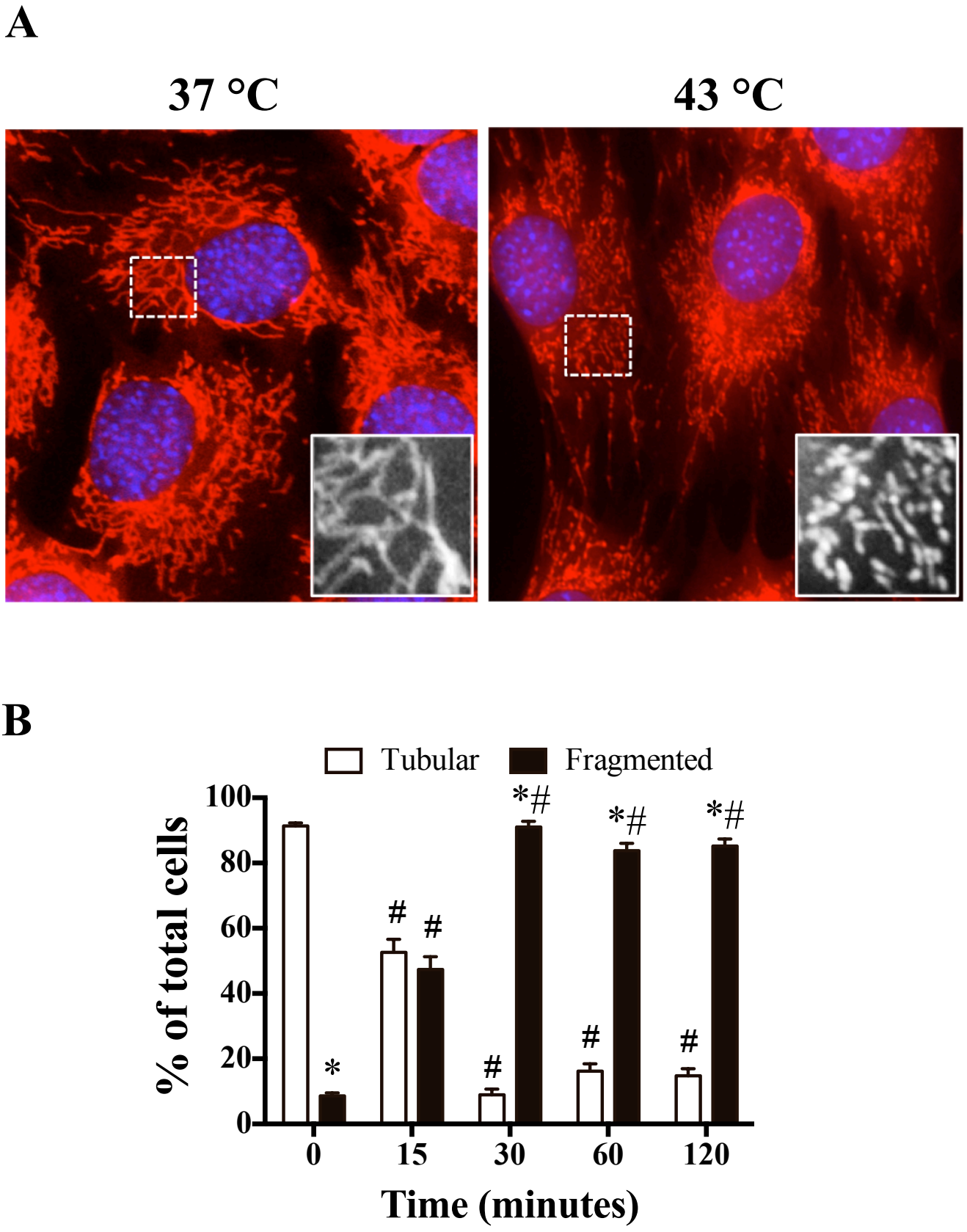
A
37 °C
43 °C
B
Tubular
Fragmented
% of total cells
100
80
60
40
20
0
*
#
#
#
*#
#
*#
#
*#
0
15
30
60
120
Time (minutes)

Figure 4

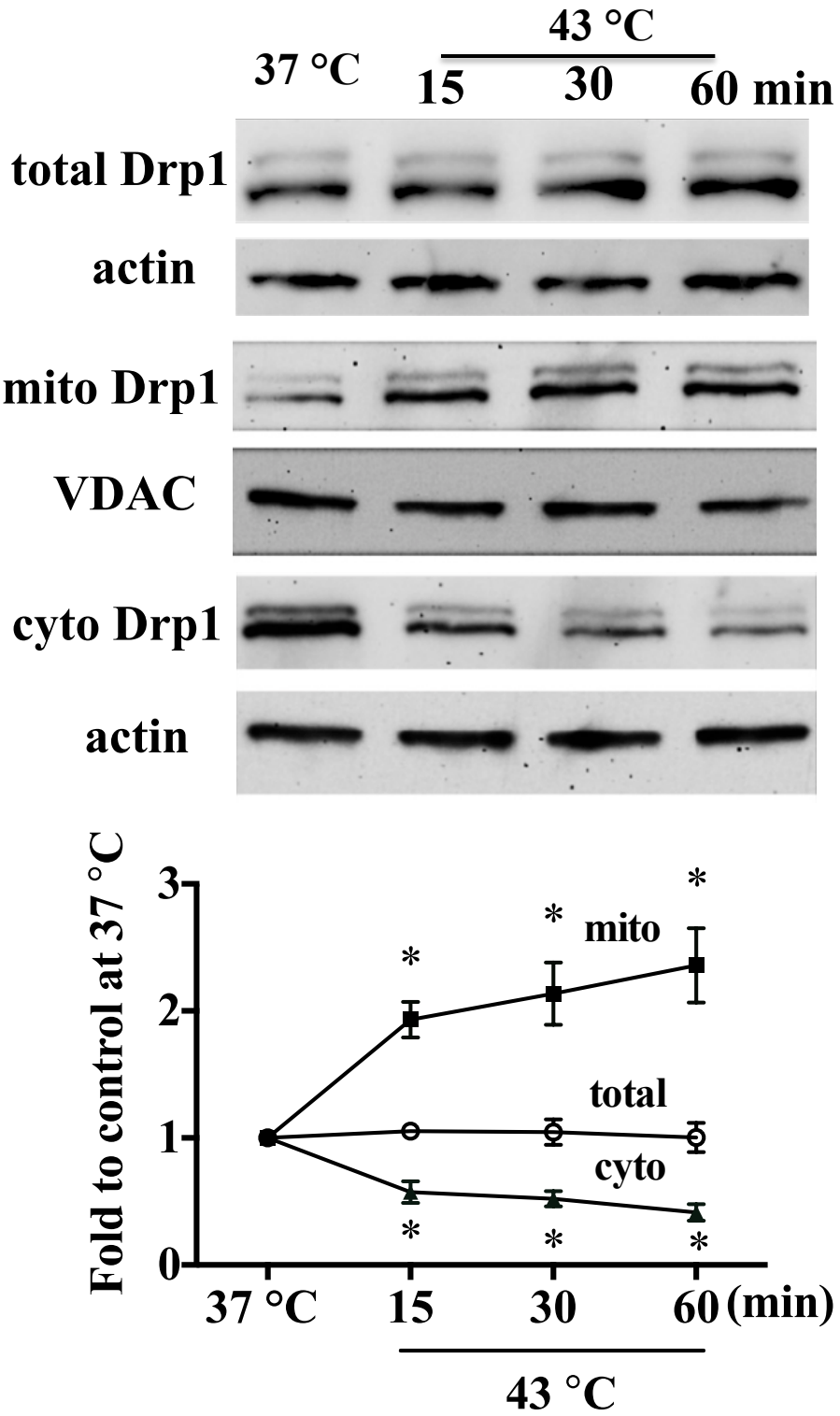
A
43 °C
37 °C
15
30
60 min
total Drp1
actin
mito Drp1
VDAC
cyto Drp1
actin
Fold to control at 37 °C
3
2
1
0
mito
total
cyto
37 °C
15
30
60 (min)
43 °C

Figure 5

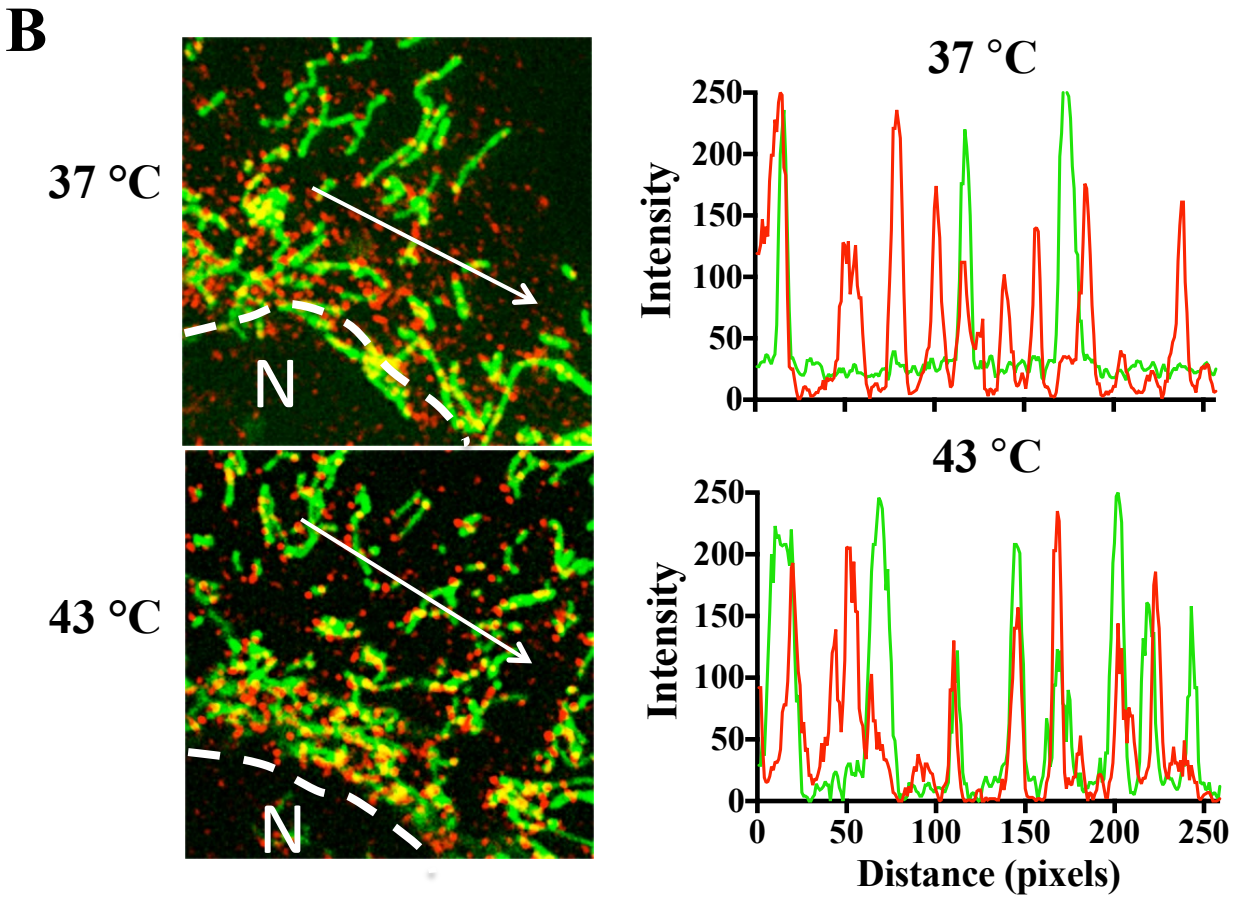
B
37 °C
43 °C
N
N
37 °C
Intensity
250
200
150
100
50
0
43 °C
Intensity
250
200
150
100
50
0
0
50
100
150
200
250
Distance (pixels)

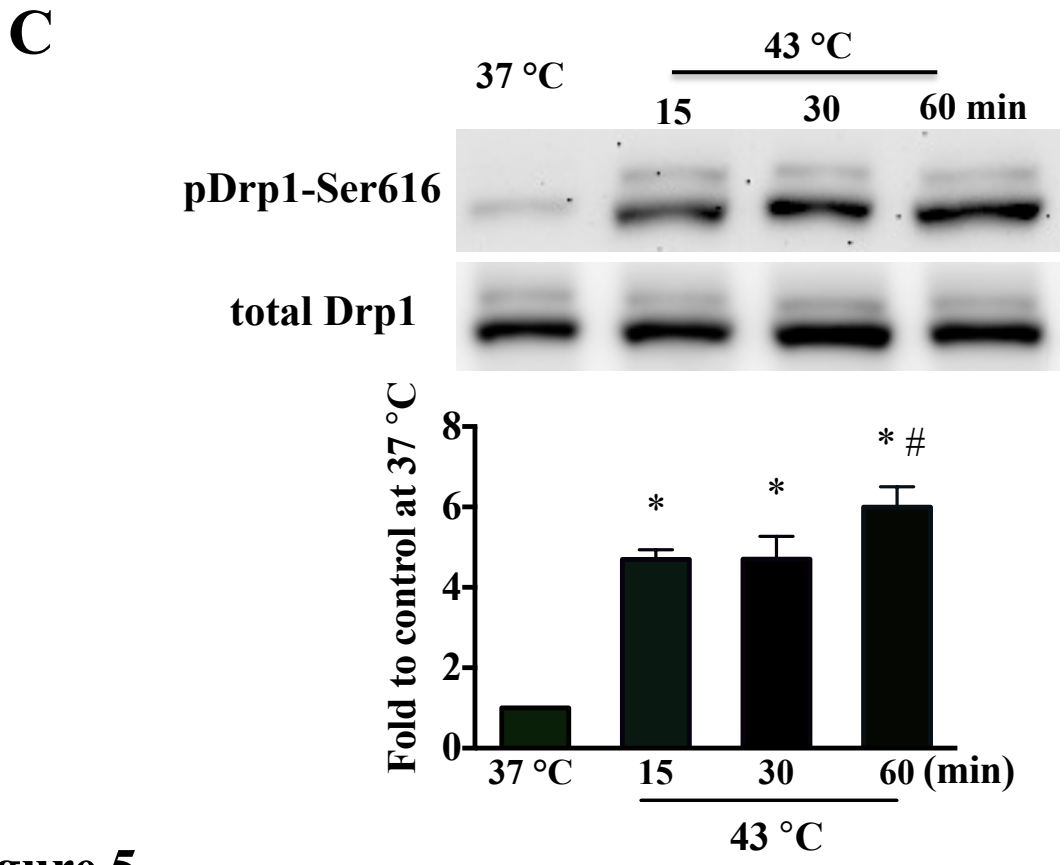
C
37 °C
43 °C
15
30
60 min
pDrp1-Ser616
total Drp1
Fold to control at 37 °C
8
6
4
2
0
*
*
* #
37 °C
15
30
60 (min)
43 °C

Figure 5

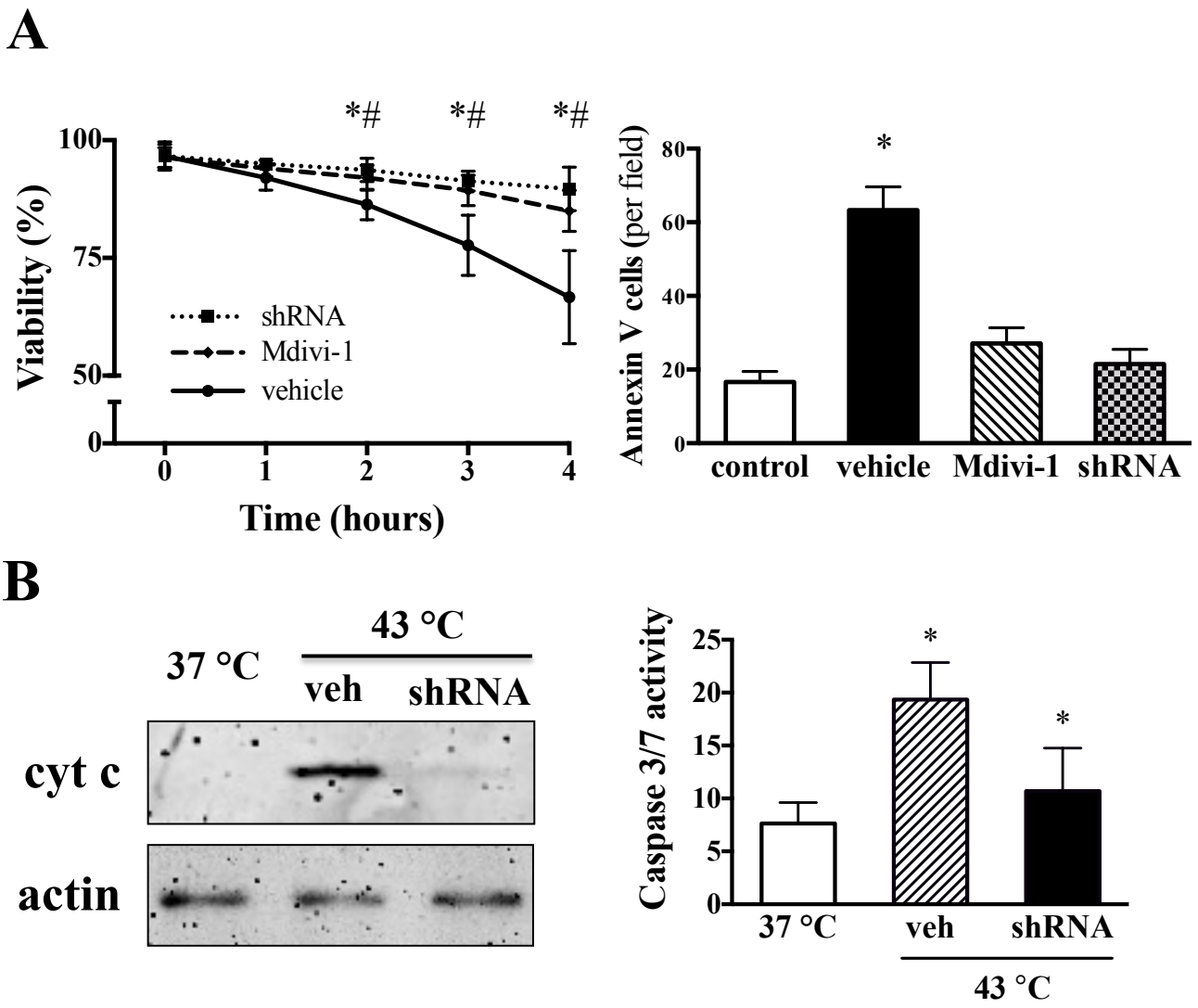
A
*#
*#
*#
100
75
50
0
Viability (%)
shRNA
Mdivi-1
vehicle
0
1
2
3
4
Time (hours)
Annexin V cells (per field)
80
60
40
20
0
*
control
vehicle
Mdivi-1
shRNA
B
37 °C
43 °C
veh
shRNA
cyt c
actin
Caspase 3/7 activity
25
20
15
10
5
0
*
*
37 °C
veh
shRNA
43 °C

Figure 6

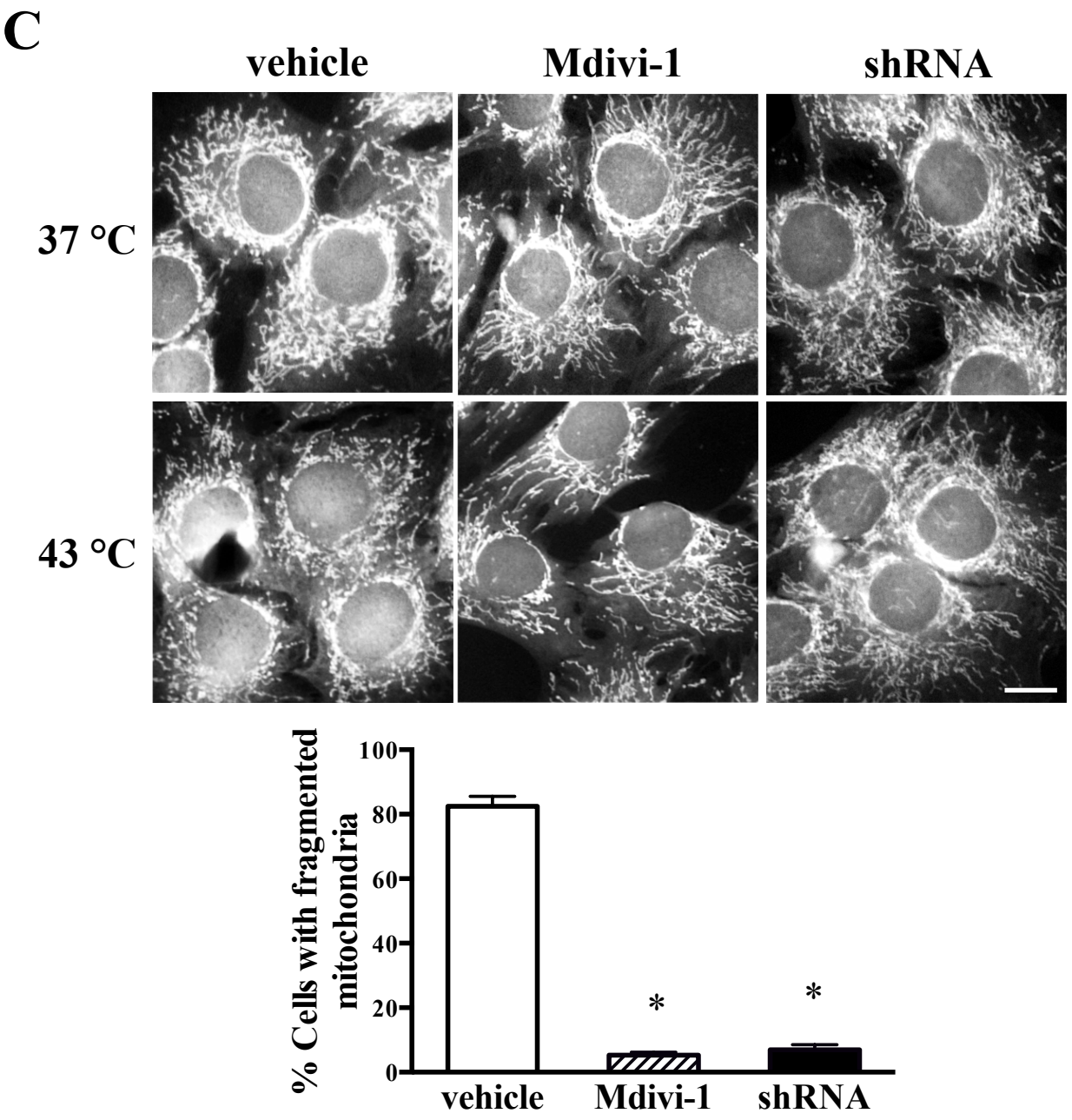
C
vehicle
Mdivi-1
shRNA
37 °C
43 °C
% Cells with fragmented mitochondria
100
80
60
40
20
0
*
*
vehicle
Mdivi-1
shRNA
D
vehicle
GFP
shRNA
Drp1
VDAC

Figure 6

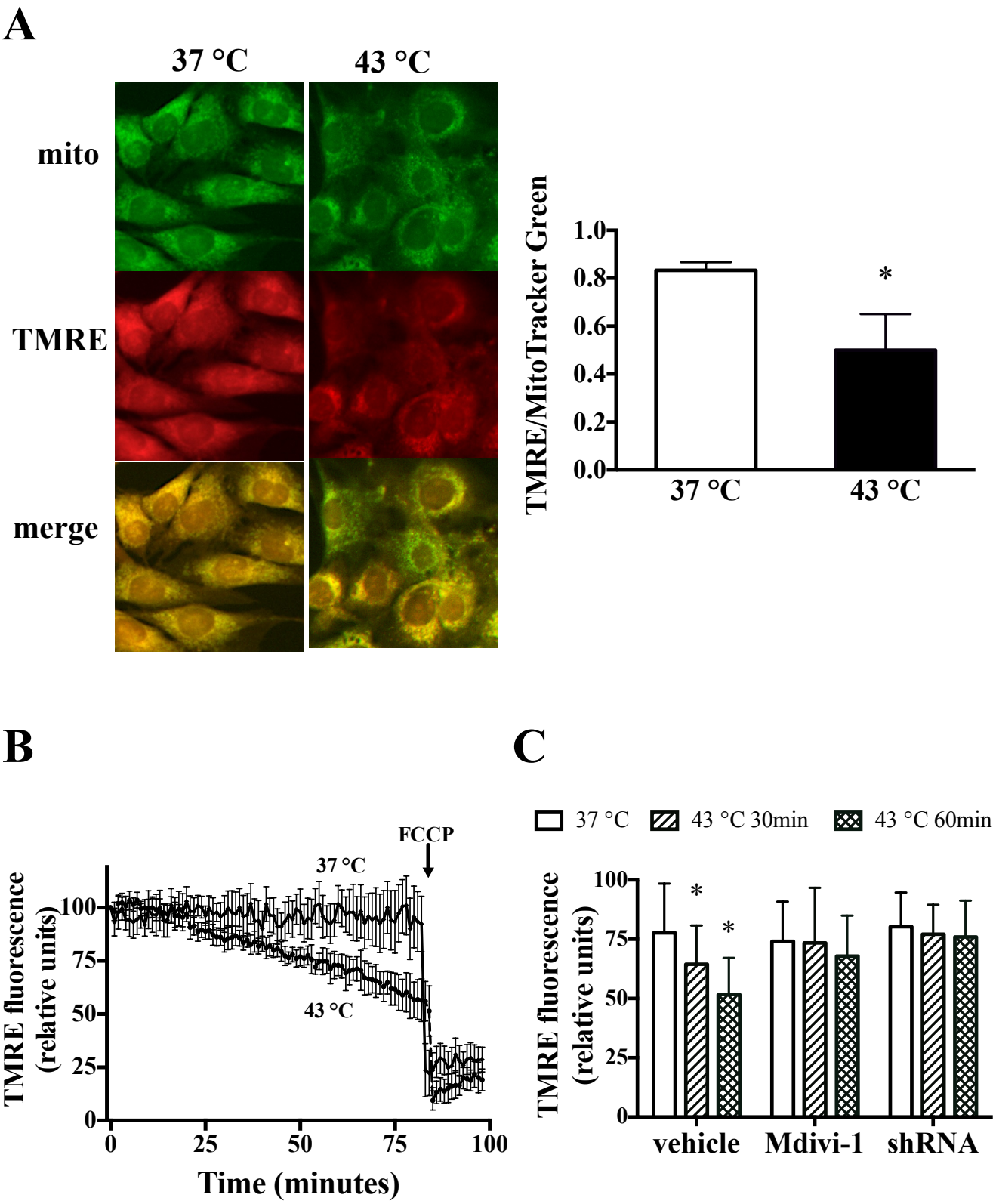
A
37 °C
43 °C
mito
TMRE
merge
TMRE/MitoTracker Green
1.0
0.8
0.6
0.4
0.2
0.0
*
37 °C
43 °C
B
FCCP
37 °C
43 °C
TMRE fluorescence (relative units)
100
75
50
25
0
0
25
50
75
100
Time (minutes)
C
37 °C
43 °C 30min
43 °C 60min
TMRE fluorescence (relative units)
100
75
50
25
0
*
*
vehicle
Mdivi-1
shRNA

Figure 7

D

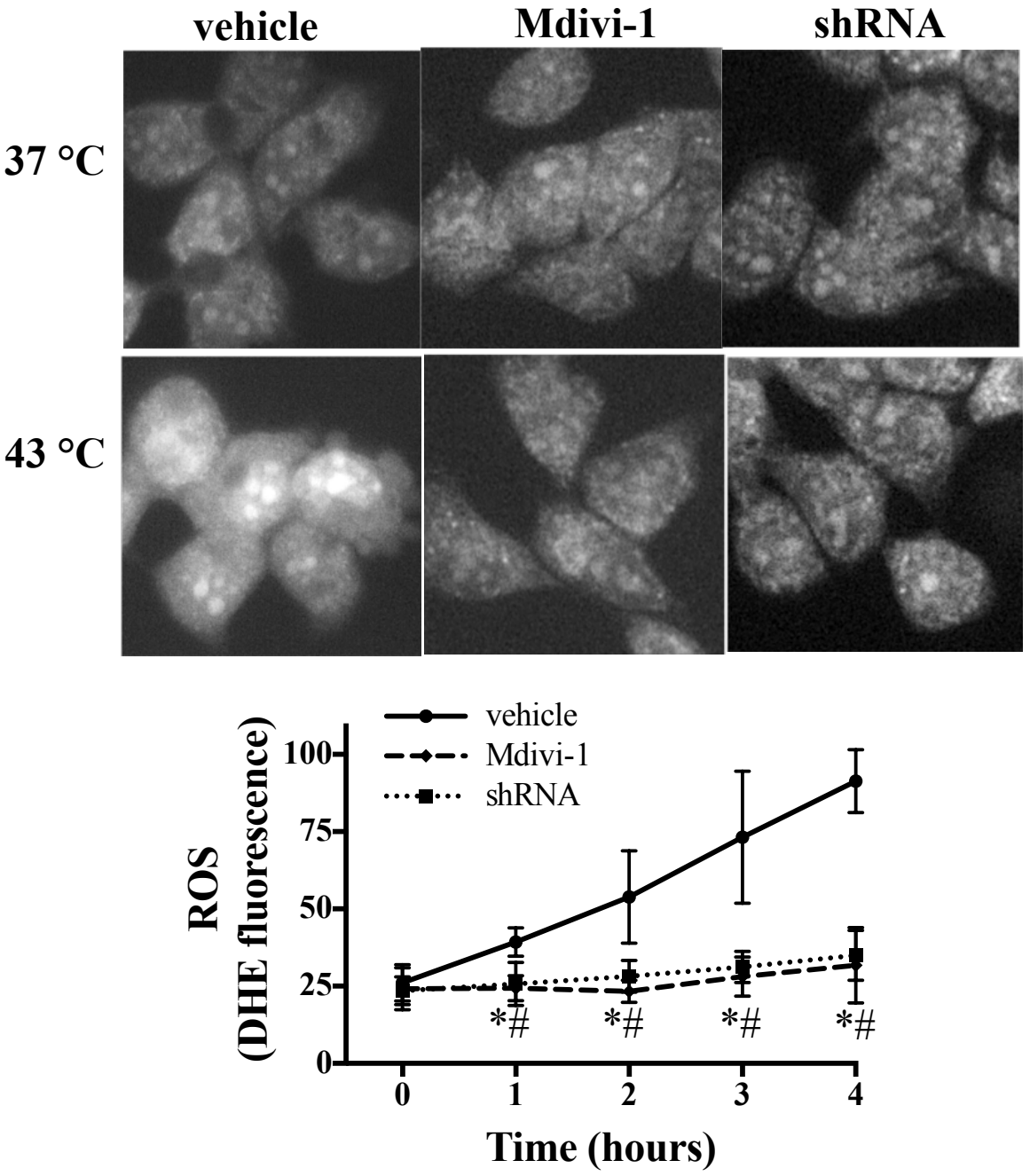
vehicle
Mdivi-1
shRNA
37 °C
43 °C
vehicle
Mdivi-1
shRNA
ROS
(DHE fluorescence)
100
75
50
25
0
*#
*#
*#
*#
0
1
2
3
4
Time (hours)

Figure 7

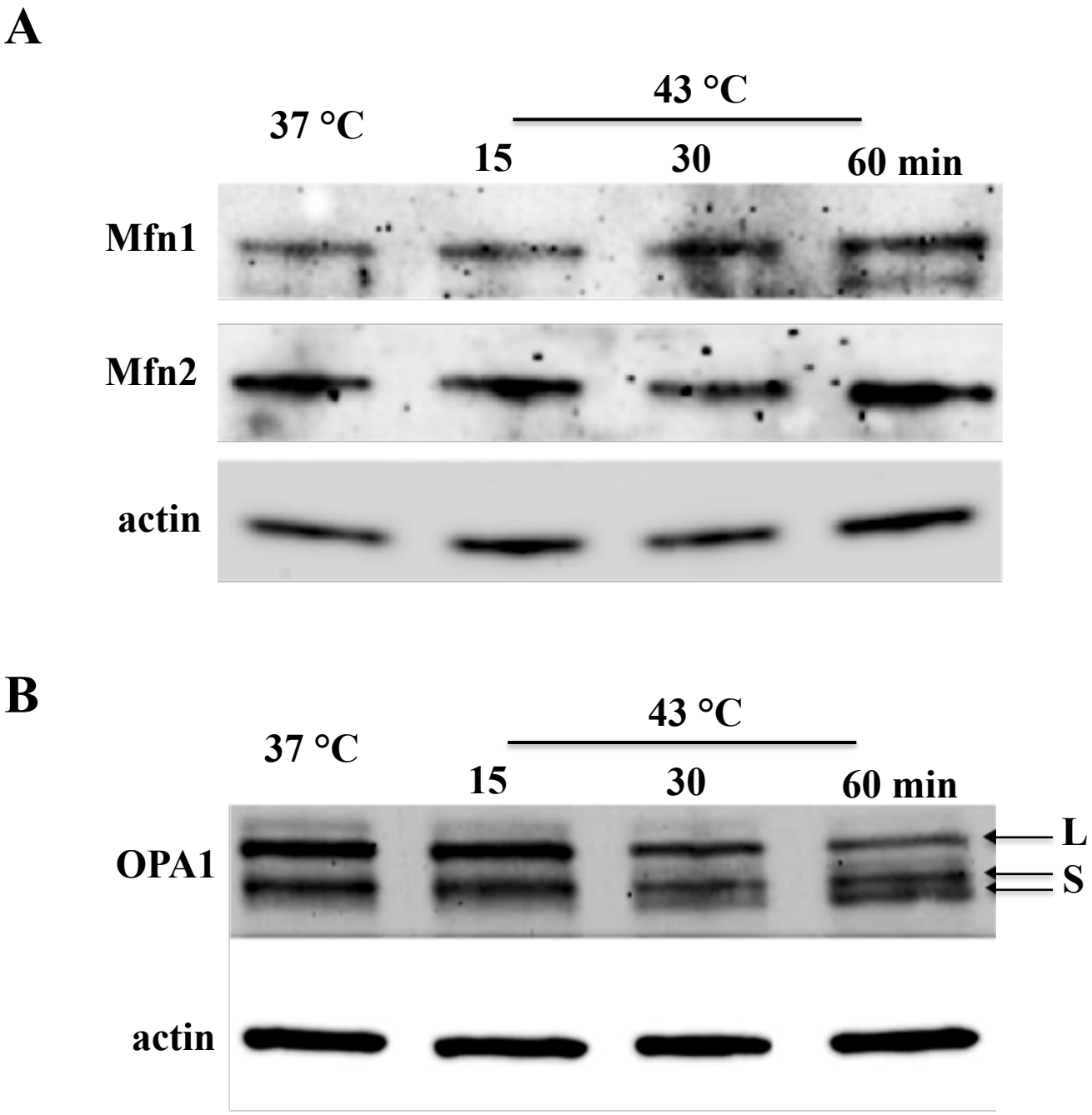
A
37 °C
43 °C
15
30
60 min
Mfn1
Mfn2
actin
B
37 °C
43 °C
15
30
60 min
OPA1
L
S
actin

Figure 8